Journal of Virology®

VIRUS-CELL INTERACTIONS

PIWIL4 Maintains HIV-1 Latency by Enforcing Epigenetically Suppressive Modifications on the 5′ Long Terminal Repeat

Zhangping He,[a] Shuliang Jing,[a] Tao Yang,[a] Jingliang Chen,[a] Feng Huang,[a] Wanying Zhang,[a] Zhilin Peng,[a] Bingfeng Liu,[a] Xiancai Ma,[a] Liyang Wu,[a] Ting Pan,[c] Xu Zhang,[a] Linghua Li,[d] Weiping Cai,[d] Xiaoping Tang,[d] Junsong Zhang,[b] Hui Zhang[a]

[a]Institute of Human Virology, Key Laboratory of Tropical Disease Control of Ministry of Education, Guangdong Engineering Research Center for Antimicrobial Agent and Immunotechnology, Zhongshan School of Medicine, Sun Yat-Sen University, Guangzhou, Guangdong, China

[b]Guangdong Provincial People's Hospital, Guangdong Academy of Medical Sciences, Guangzhou, Guangdong, China

[c]School of Medicine, Sun Yat-Sen University, Guangzhou, Guangdong, China

[d]Department of Infectious Diseases, Guangzhou Eighth People's Hospital, Guangzhou Medical University, Guangzhou, Guangdong, China

ABSTRACT Although substantial progress has been made in depicting the molecular pathogenesis of human immunodeficiency virus type 1 (HIV-1) infection, the comprehensive mechanism of HIV-1 latency and the most promising therapeutic strategies to effectively reactivate the HIV-1 latent reservoir to achieve a functional cure for AIDS remain to be systematically illuminated. Here, we demonstrated that piwi (P element-induced Wimpy)-like RNA-mediated gene silencing 4 (PIWIL4) played an important role in suppressing HIV-1 transcription and contributed to the latency state in HIV-1-infected cells through its recruitment of various suppressive factors, including heterochromatin protein 1$\alpha/\beta/\gamma$, SETDB1, and HDAC4. The knockdown of PIWIL4 enhanced HIV-1 transcription and reversed HIV-1 latency in both HIV-1 latently infected Jurkat T cells and primary CD4$^+$ T lymphocytes and resting CD4$^+$ T lymphocytes from HIV-1-infected individuals on suppressive combined antiretroviral therapy (cART). Furthermore, in the absence of PIWIL4, HIV-1 latently infected Jurkat T cells were more sensitive to reactivation with vorinostat (suberoylanilide hydroxamic acid, or SAHA), JQ1, or prostratin. These findings indicated that PIWIL4 promotes HIV-1 latency by imposing repressive marks at the HIV-1 5′ long terminal repeat. Thus, the manipulation of PIWIL4 could be a novel strategy for developing promising latency-reversing agents (LRAs).

IMPORTANCE HIV-1 latency is systematically modulated by host factors and viral proteins. During this process, the suppression of HIV-1 transcription plays an essential role in promoting HIV-1 latency. In this study, we found that PIWIL4 repressed HIV-1 promoter activity and maintained HIV-1 latency. In particular, we report that PIWIL4 can regulate gene expression through its association with the suppressive activity of HDAC4. Therefore, we have identified a new function for PIWIL4: it is not only a suppressor of endogenous retrotransposons but also plays an important role in inhibiting transcription and leading to latent infection of HIV-1, a well-known exogenous retrovirus. Our results also indicate a novel therapeutic target to reactivate the HIV-1 latent reservoir.

KEYWORDS epigenetics, HDAC4, HIV-1 latency, PIWIL4

Despite suppressive combination antiretroviral therapy (cART), a pool of long-lived central memory CD4$^+$ T lymphocytes, which stably harbor replication-competent but transcriptionally silenced proviruses, represents a major obstacle to a definitive cure for HIV-1 infection (1–4). Because of the stability of the HIV-1 latent reservoir, lifelong treatment is required, and the accompanying occurrence of different adverse effects of this treatment compromises life quality. The "shock and kill" strategies have failed to

Citation He Z, Jing S, Yang T, Chen J, Huang F, Zhang W, Peng Z, Liu B, Ma X, Wu L, Pan T, Zhang X, Li L, Cai W, Tang X, Zhang J, Zhang H. 2020. PIWIL4 maintains HIV-1 latency by enforcing epigenetically suppressive modifications on the 5′ long terminal repeat. J Virol 94:e01923-19. https://doi.org/10.1128/JVI.01923-19.

Editor Guido Silvestri, Emory University

Address correspondence to Junsong Zhang, zhangjuns_0953@163.com, or Hui Zhang, zhangh92@mail.sysu.edu.cn.

Received 13 November 2019
Accepted 21 February 2020
Accepted manuscript posted online 11 March 2020
Published 4 May 2020

efficiently purge the viral reservoir so far (5–9). Hence, the mechanisms for establishing and maintaining HIV-1 latency *in vivo* and reactivating the viral reservoir need to be further illuminated, especially from the perspective of epigenetic modulation.

Epigenetic modulation is extensively involved in the establishment and maintenance of HIV-1 latency. Several types of "writers and erasers" responsible for the formation of repressive histone marks were reported to be associated with the HIV-1 5′ long terminal repeat (LTR) region, including a variety of histone methyltransferases (e.g., GLP, G9a, Suv39H1, EZH2, and SMYD2) and histone deacetylases (e.g., HDAC1 to -4) (10–18). It was reported that these repressive epigenetic marks were further maintained by the "readers," such as HP1$\alpha/\beta/\gamma$ and Trim28 (15, 19, 20). Both histone methylation (e.g., H3K9 di- and trimethylation [H3K9me2/3], H3K27me3, and hypoacetylation) and HP1$\alpha/\beta/\gamma$ recruitment lead to repressive chromatin conformation and the formation of heterochromatin (21). Recently, Sad1 and UNC84 domain-containing 2 (SUN2) and scaffold attachment factor B (SAFB1) were reported to inhibit HIV-1 transcription through the maintenance of repressive chromatin at the HIV-1 promoter and blocking the recruitment of phosphorylated RNA polymerase II to the promoter, respectively (22, 23). In addition, the long noncoding RNA MALAT1 (metastasis-associated lung adenocarcinoma transcript 1) was reported by the same group to release epigenetic silencing of the HIV-1 LTR by antagonizing the binding of polycomb complex 2 (PRC2) to the HIV-1 5′ LTR (24).

Belonging to the Argonaute (AGO) protein family, PIWI subfamily members are well characterized and defined by the presence of the PAZ (PIWI–AGO-Zwille) domain, located within the N-terminal region and responsible for RNA binding, as well as the presence of the PIWI domain, located in the C-terminal region with RNase endonuclease activity specifically for double-stranded RNA (25, 26). The human PIWI family consists of four PIWI proteins: PIWIL1 (Hiwi), PIWIL2 (Hili), PIWIL3 (Hiwi3), and PIWIL4 (Hiwi2). Compared to the human genome, three homologous counterparts of human PIWI proteins are detectable in the mouse genome (PIWIL1 [Miwi], PIWIL2 [Mili], and PIWIL4 [Miwi2]), with the exception of PIWIL3 (27). Three PIWI homologues, namely, PIWI, Aubergine (AUB), and AGO3, were characterized in the fruit fly (28). Although it has been reported that loading with PIWI-interacting RNA (piRNA) is important for the nuclear entry of PIWI proteins (29, 30), whether free PIWI proteins without piRNA loading could exist in the nucleus is unclear.

piRNAs are 26- to 31-nucleotide small noncoding RNAs that are characterized as being associated with PIWI proteins and modified with 2′-*O*-methyl at their 3′ termini. piRNAs are generated from transposons and were previously considered exclusively germ line expressed (31–35). Their generation and function are coupled by a "ping-pong cycle" in germ cells (36, 37). For a long time, germ line cells have been considered a major location for piRNA to exert its inhibitory function upon transposons. However, growing evidence has indicated that piRNAs or piRNA-like molecules, which are basically generated from further cleavage of tRNA or small nucleolar RNA (snoRNA), are widely expressed in human somatic and cancer cells. These tRNA-derived piRNAs are more frequently referred to as tRNA-derived RNA fragments (tRFs). It is notable that these tRNA- or snoRNA-derived piRNAs or piRNA-like molecules are associated with PIWI proteins, indicating that their function is coupled with those of PIWI proteins (38, 39). It is now clear that PIWI-associated piRNAs or piRNA-like molecules not only are transposon silencers in germ line cells but also regulate the expression of various genes in somatic cells under certain physiological and pathological processes (40–46). Most recently, it was reported that the processing of sense piRNAs from unspliced KoRV-A (koala retrovirus subtype A) transcripts is the preferential response to the retroviral invasion into the koala germ line genome (47). Furthermore, this piRNA process pattern is deeply conserved among transposons from insects to placental mammals (47). It has long been known that PIWIL4 can increase the methylation of H3K9 at the $p16^{Ink4a}$ (CDKN2A) locus in human somatic cell lines, indicating that PIWIL4 functions in the chromatin-modifying pathway (48, 49). Our previous works also have shown that human PIWIL4 plays an important role in modulating gene expression in immune cells

in a snoRNA- or tRNA-derived piRNA-dependent manner (39, 50). We and others have also shown that PIWIs in somatic cells are recruited to gene loci via the complementary recognition of PIWI-associated piRNAs and the targeted chromatin regions or the nascent mRNA they transcribed (39, 51, 52). In most cases, the PIWI/piRNA complex is recruited to the gene loci to suppress gene expression, although gene activation also can be identified (46).

Transposable elements (TEs) account for nearly half the human genome, most of which are retrotransposons. *Alu* elements are among the most abundant retrotransposons (53, 54). The expression of *Alu* RNA is negatively regulated by nuclear PIWIL4 through epigenetic downregulation and heterochromatin formation. PIWI family members negatively regulate gene expression through different mechanisms (49). They can not only modulate gene expression at the transcription level, by inducing DNA methylation at the promoter region or by inducing repressive histone methylation followed by heterochromatin formation at the target gene loci, but also mediate mRNA degradation at posttranscriptional level (39, 50, 51, 55). The cytoplasmic sequestration of PIWIL4 causes the accumulation of *Alu* RNA in retinal pigment epithelial (RPE) cells due to oxidative stress (56).

HIV-1 is an exogenous retrovirus that stably integrates into chromosomal DNA following the infection of its target cells. Postintegration latency occurs at the early phase of productive infection. Because HIV-1 provirus shares some conserved genetic elements with endogenous retroviruses, it is reasonably assumed that the expression of HIV-1 also is modulated by PIWI/piRNA. To test this hypothesis, we knocked down PIWIL4 in HIV-1 latently infected cells and demonstrated that PIWIL4 depletion reactivated HIV-1 transcription in latently infected Jurkat T cells and primary $CD4^+$ T lymphocytes. We have also demonstrated that PIWIL4 was associated with the HIV-1 5′ LTR and suppressed its activity by recruiting various repressive histone modifiers, consequently inducing the formation of suppressive histone marks and condensed chromatin conformation.

RESULTS

PIWIL4 inhibits HIV-1 replication through repressing the HIV-1 5′ LTR activity. To elucidate the roles of PIWI proteins in the HIV-1 life cycle, we analyzed the expression of PIWI proteins in resting and activated human $CD4^+$ T lymphocytes as well as in an HIV-1 latently infected T-cell line, termed J-lat 10.6, which was derived from the Jurkat T-lymphoma cell line. We found that PIWIL4 was most abundant of human PIWI proteins in all tested cells, which was in line with our previous report (Fig. 1A) (50). Contrary to PIWIL2, PIWIL4 was detected and constitutively expressed in both resting and activated $CD4^+$ T lymphocytes (Fig. 1B) (57). To study the effect of PIWIL4 upon HIV-1 replication, we used the replication-competent HIV-1_{NL4-3} strain to infect activated primary $CD4^+$ T lymphocytes after depletion of PIWIL4 using a PIWIL4-specific small interfering RNA (siRNA) combination. The effective knockdown of endogenous PIWIL4 in activated primary $CD4^+$ T lymphocytes was confirmed (Fig. 1C and D). We found that the knockdown of PIWIL4 increased HIV-1/NL4-3 replication in primary $CD4^+$ T lymphocytes (Fig. 1E), suggesting that endogenous PIWIL4 suppressed HIV-1 replication. To investigate the underlying mechanisms, we analyzed the effect of PIWIL4 on HIV-1 promoter activity in TZM-b1 cells (58, 59). We knocked down endogenous PIWIL4 in TZM-bl cells by using PIWIL4-specific siRNAs. The depletion efficiency of the single PIWIL4-specific siRNA used here was confirmed at mRNA and protein expression levels (Fig. 1F and G), and we found that PIWIL4 depletion increased integrated 5′ LTR-driven expression 2.1- to 2.4-fold or 4.3- to 4.5-fold in the absence or presence of Tat, respectively (Fig. 1H) (60–62). When we treated the TZM-bl cells with tumor necrosis factor alpha (TNF-α), the stimulated gene expression was also significantly enhanced by PIWIL4 depletion (Fig. 1H) (63). Further, we observed similar results with cotransfection assays in HeLa cells using the dual-luciferases reporter assay system. This system expresses *renilla* luciferase driven by the cytomegalovirus promoter as a normalized control and *firefly* luciferase driven by the full-length 5′ LTR of HIV-1/NL4-3 with

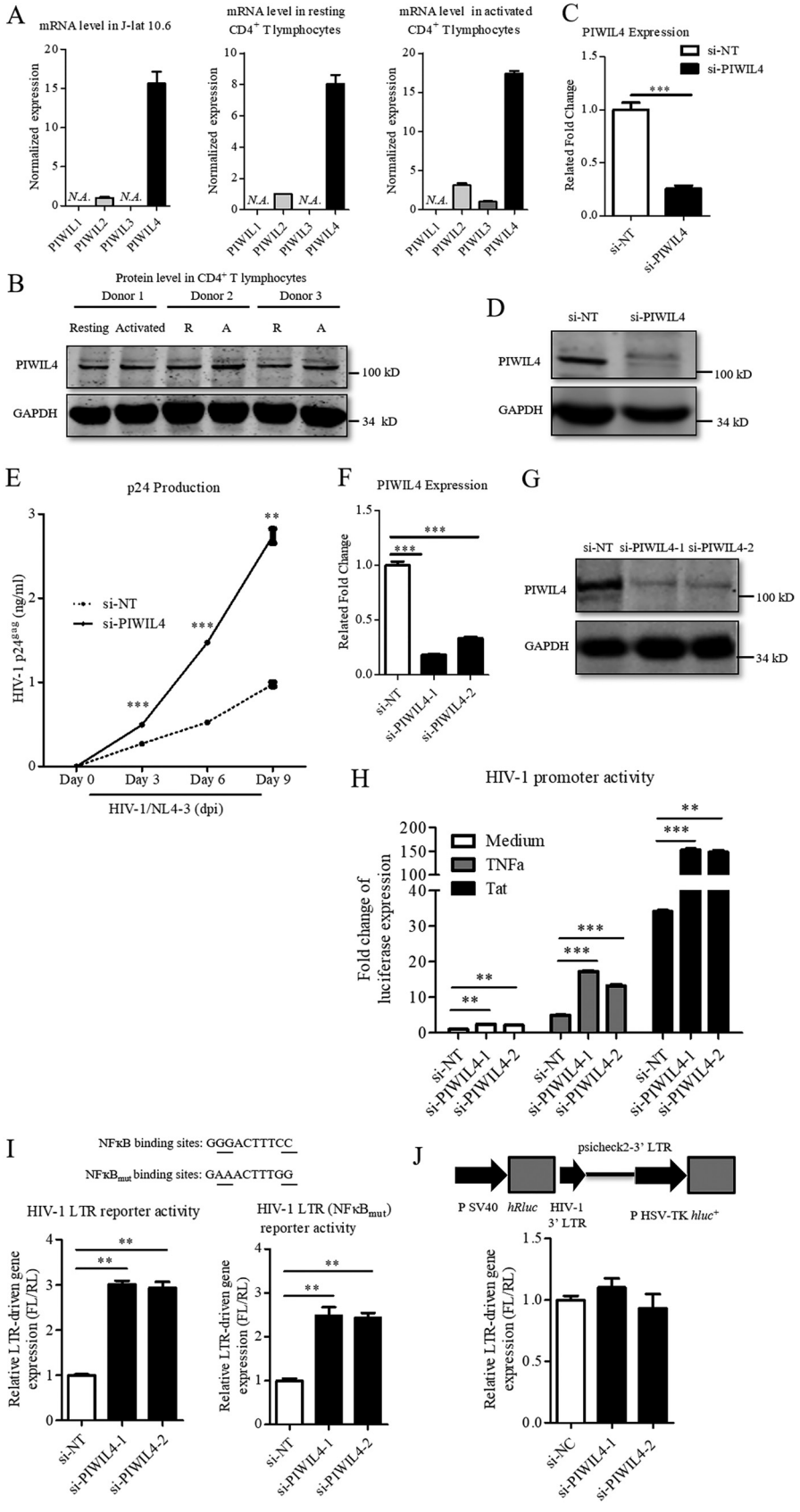

FIG 1 PIWIL4 inhibits HIV-1 replication through repressing the HIV-1 5′ LTR activity. (A) The relative expression of human PIWIs in resting and activated CD4$^+$ T lymphocytes as well as in J-lat 10.6 cells was

(Continued on next page)

two consecutive mutated NF-κB binding sites (64). We found that PIWIL4 still inhibited 5′ LTR activity when the mutations of the NF-κB binding sites were generated, indicating that PIWIL4 inhibition of HIV-1 transcription is independent from the NF-κB signaling pathway (Fig. 1I). It is notable that there are two identical LTRs located upstream and downstream of the firefly luciferase in TZM-bl cells. To rule out the possibility that the activity of the 3′ LTR was influenced by PIWIL4, we cloned the 3′ LTR into an si-check-2 vector as the 3′ untranslated region (UTR) of the *renilla* luciferase transcript. We found that the amount of *renilla* luciferase in HeLa cells showed no obvious difference between the PIWIL4 depletion group and its nontarget control (Fig. 1J). Taken together, these results indicated that PIWIL4 inhibited HIV-1 replication by suppressing HIV-1 5′ LTR activity.

PIWIL4 promotes HIV-1 latency in HIV-1-infected Jurkat cells. The repression of HIV-1 5′ LTR activity by PIWIL4 suggested its intrinsic role in HIV-1 latency. Thus, we sought to investigate the effect of PIWIL4 depletion on the expression of a single integrated provirus of the HIV-1 latently infected cell lines, J-lat 10.6 and J-lat 8.4 (65). HIV-1 reactivation in these cell lines could be indicated by quantifying green fluorescent protein (GFP) expression (66). First, the knockdown efficiency of PIWIL4-specific short hairpin RNA (shRNA) was confirmed (Fig. 2A and B). We observed a significant reactivation of HIV-1 in J-lat 10.6 and J-lat 8.4 cells after the knockdown of PIWIL4 by PIWIL4-specific shRNA (Fig. 2C and D). Given that no single agent met the requirement of effectively "shocking" the HIV-1 latent reservoir, it is important to develop multifunctional latency-reversing agents (LRAs) and/or novel candidates that could significantly enhance HIV-1 reactivation upon stimulation with commonly used LRAs, such as suberoylanilide hydroxamic acid (SAHA), JQ1, or prostratin (19, 67, 68). Thus, we assessed HIV-1 reactivation upon PIWIL4 depletion in the presence of various LRAs. The knockdown of PIWIL4 significantly enhanced HIV-1 reactivation upon stimulation with SAHA, JQ1, or prostratin compared to that of the controls (Fig. 2C and D). Both the percentage and mean fluorescence intensity (MFI) of the GFP expression from J-lat 10.6 cells (Fig. 2E) and J-lat 8.4 cells (Fig. 2F) were significantly increased after PIWIL4 depletion in the absence or presence of individual LRAs, including SAHA, JQ1, or prostratin. Accordingly, the DNA methylation inhibitor decitabine notably enhanced the reactivation of J-lat 8.4 cells when PIWIL4 was depleted (Fig. 2D). These results suggested that endogenous PIWIL4 mediated the suppression of HIV-1 proviral DNA expression and established and maintained HIV-1 latency in $CD4^+$ T lymphocytes.

PAZ domain is required for PIWIL4 to be associated with the HIV-1 5′ LTR. It has been known that PIWIL4-piRNA could be recruited to the promoter region of target genes to modulate gene expression (39). To investigate whether PIWIL4 could interact

FIG 1 Legend (Continued)
detected by quantitative RT-PCR (qRT-PCR), and results were normalized to the expression of *GAPDH*. (B) The expression of PIWIL4 in resting and activated $CD4^+$ T lymphocytes from three different healthy donors was examined by immunoblotting. (C to E) Anti-CD3/CD28 antibody-stimulated primary $CD4^+$ T lymphocytes from healthy donors were transfected with PIWIL4-specific siRNAs (si-PIWIL4) or nontarget control (si-NT). (C and D) The cells were collected at 48 h posttransfection, and PIWIL4 expression was determined by qRT-PCR and immunoblotting. (E) Cells were infected with replication-competent HIV-1/NL4-3. The levels of HIV-1 p24 in the supernatants were quantified by ELISA. dpi, days postinfection. (F to H) TZM-bl cells were transfected with si-PIWIL4 or si-NT. The efficiency of endogenous PIWIL4 knockdown by the indicated siRNAs was confirmed by qRT-PCR and immunoblotting (F and G), and cells were jointly transfected with HIV-1 Tat-expressing vector or treated with TNF-α (50 ng/ml for 24 h) (H). Cells were harvested and assayed for luciferase. The quantitation was normalized to the si-NT. (I) The wild-type or NF-κB-binding site-mutated HIV-1 5′ LTR cloned from pNL4-3 was inserted into a pGL3 basic vector. The endogenous PIWIL4 in HeLa cells was knocked down by specific siRNAs. After 12 h, these cells were further transfected with the wild type or mutated LTR promoter-driven luciferase reporter plasmid for an additional 36 h, harvested, and assayed for luciferase. The quantitation was normalized to the si-NT. (J) The 3′ LTR cloned from pNL4-3 was inserted into a psi-check-2 vector. The endogenous PIWIL4 in HeLa cells was knocked down by specific siRNAs. After 12 h, cells were further transfected with this newly constructed reporter plasmid for an additional 36 h. The firefly luciferase driven by the HSV-TK promoter was used to normalize transfection efficiency. Cells were harvested and luciferase expression was assayed. The quantitation was normalized to the si-NT. Results are representative of three independent experiments. Data are presented as means ± SEM. *P* values were calculated by Student's *t* test. **, $P < 0.01$; ***, $P < 0.001$.

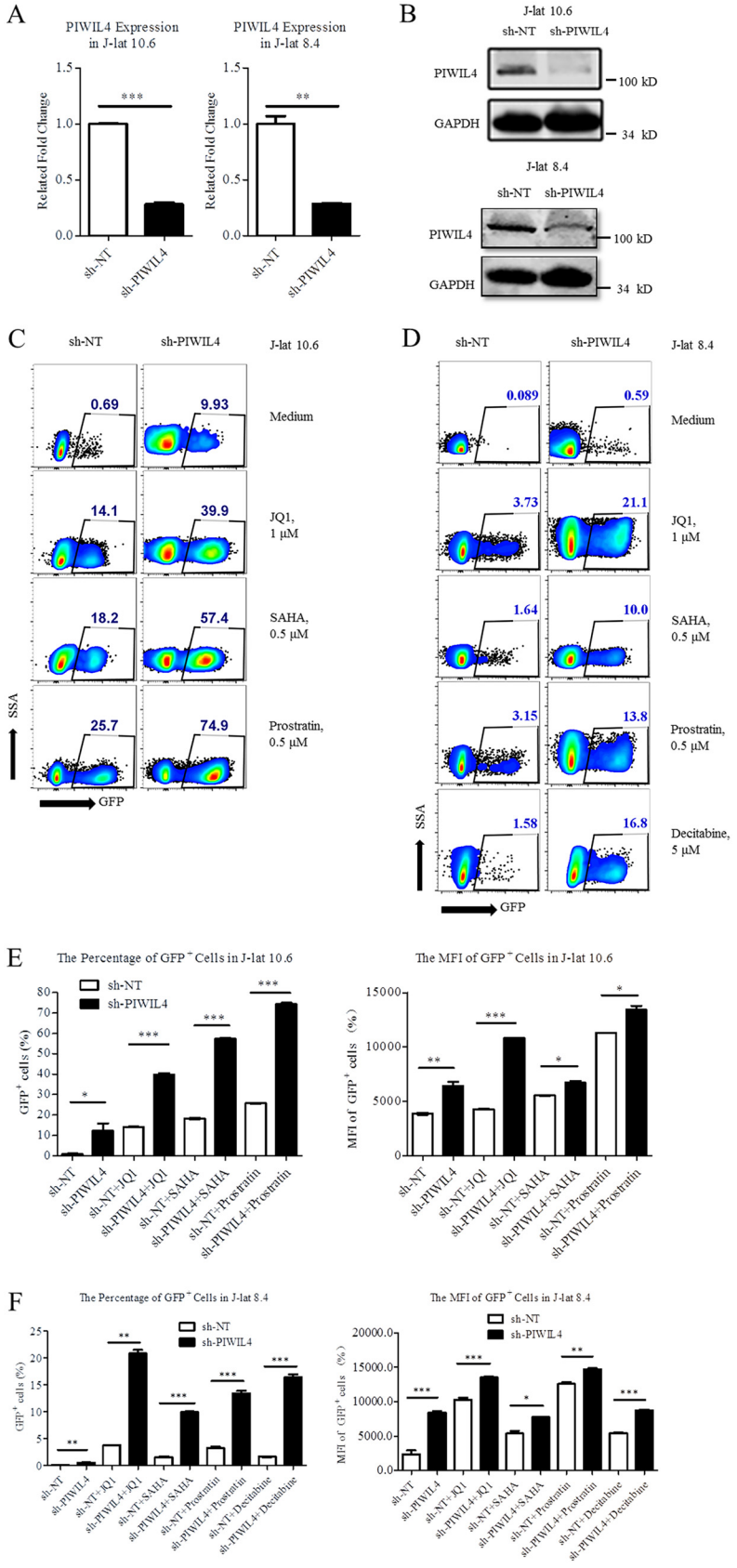

FIG 2 PIWIL4 promotes HIV-1 latency in HIV-1-infected Jurkat cells. The shRNA constructs were packaged into VSV-G-pseudotyped lentivectors and transduced into J-lat 10.6 and 8.4 cells for 4 days. (A and B)

(Continued on next page)

with the integrated HIV-1 proviral DNA, we performed a chromatin immunoprecipitation-quantitative PCR (ChIP-qPCR) assay with a PIWIL4-specific antibody and various primers for HIV-1 within J-lat 10.6 (20). We found that endogenous PIWIL4 specifically associated with the LTR region of the integrated HIV-1 genome in J-lat 10.6 cells (Fig. 3A). There are three consecutive nucleosomes located both upstream and downstream of the HIV-1 5′ LTR, termed Nuc-0, Nuc-1, and Nuc-2 (69). To further explore the specific region of 5′ LTR associated with PIWIL4, we conducted a ChIP-qPCR assay with five primer pairs located within different sites of the HIV-1 LTR and the adjacent *gag* leader sequence (GLS) (Fig. 3B). We observed gradual enhancement of PIWIL4 association with the HIV-1 5′ LTR from the 5′ terminus of the U3 region to the 3′ end of the U5 region and the adjacent GLS (Fig. 3C). In addition, when we repeated the ChIP-qPCR assays in TZM-bl cells in the presence of PIWIL4-specific siRNA, similar results were observed (Fig. 3D). These results indicated that PIWIL4 was associated with the 5′ LTR of integrated HIV-1 proviral DNA within the region between Nuc-1 and Nuc-2.

PIWIL4 contains two major domains, PAZ and PIWI. Seven nonconsecutive sites distributed inside the PAZ domain are responsible for its binding to piRNAs (70, 71). The abnormal piRNA binding affinity of PIWIL4 would abolish the association of PIWIL4 with piRNAs and restrict its nuclear entry and gene locus targeting. Previous studies showed that the silencing of genetic elements mediated by the PIWI/piRNA complexes was mainly a nuclear process (52, 72). To explore whether the nuclear entry or HIV-1 5′ LTR-targeting activity of PIWIL4 is indispensable for HIV-1 5′ LTR repression, we constructed six sequentially truncated PIWIL4 mutants with an overlap of at least 20 amino acids between the adjacent mutants. All mutants, as well as wild-type PIWIL4, were labeled with a hemagglutinin (HA) tag at their N termini. Specifically, the PIWIL4-Δ262-401 mutant lacked nearly the whole PAZ domain, and the PIWIL4-Δ562-705 and PIWIL4-Δ756-852 mutants each lost half of the PIWI domain, respectively. Besides these truncated mutants, we also generated a PIWIL4 mutant (PIWIL4-PAZ_{mut}) to abolish its binding affinity to piRNA by mutating all known piRNA binding sites, including D315A, K328A, Y336A, Y340A, S358A, A373S, and L375Y (70, 71). To restore the nuclear entry ability of the PIWIL4-PAZ_{mut}, we inserted a nuclear localization signal from SV40 into the PIWIL4 coding DNA sequence (NLS_{SV40}-PIWIL4-PAZ_{mut}) (Fig. 3E and F). All PIWIL4 mutants were expressed normally in TZM-bl cells (Fig. 3G). We then performed the ChIP-qPCR assays with the TZM-bl V5 primer pair and found that the mutants without an intact PAZ domain lost their association with the HIV-1 5′ LTR, and the addition of NLS_{SV40} did not restore this association (Fig. 3G).

To determine whether the inhibitory effect on HIV-1 transcription by PIWIL4 is dependent on its nuclear translocation and/or association with the targeted chromatin regions when binding to piRNA as a complex, we performed the transfection assay in TZM-bl cells. Unlike siRNA-resistant wild-type (WT) PIWIL4, PIWIL4-PAZ_{mut} did not restore the repression activity of the 5′ LTR by knockdown of endogenous PIWIL4 in TZM-bl cells (Fig. 3H and I), suggesting that the PIWIL4-mediated suppression of HIV-1 LTR activity is dependent on its association with piRNA (Fig. 3J). Thus, these results indicated that the PAZ domain is required for PIWIL4 to associate with the HIV-1 5′ LTR and repress its activity.

HIV-1 latency is enforced by PIWIL4 via its mediation of the repressive H3K9 modification on the HIV-1 5′ LTR. PIWIL4 can interact with overexpressed HP1β,

FIG 2 Legend (Continued)
mRNA expression and protein expression between sh-NT-transduced cells and those with PIWIL4 knockdown mediated by sh-PIWIL4 were compared by qRT-PCR and immunoblotting assays. (C and D) The sh-NT- and sh-PIWIL4-transduced cells were further treated with the indicated LRAs with shown concentrations for an additional 24 h, with the exception of decitabine (96 h for J-lat 8.4 cells), and HIV-1 reactivation was measured by the percentage and mean immunofluorescence intensity (MFI) of GFP^+ cells as analyzed by flow cytometry. (E and F) HIV-1 reactivation measured in panels C and D was summarized and analyzed. The results are representative of at least three independent experiments. Data represent means ± SEM from triplicates. *P* values were calculated by Student's *t* test. **, $P < 0.01$; ***, $P < 0.001$.

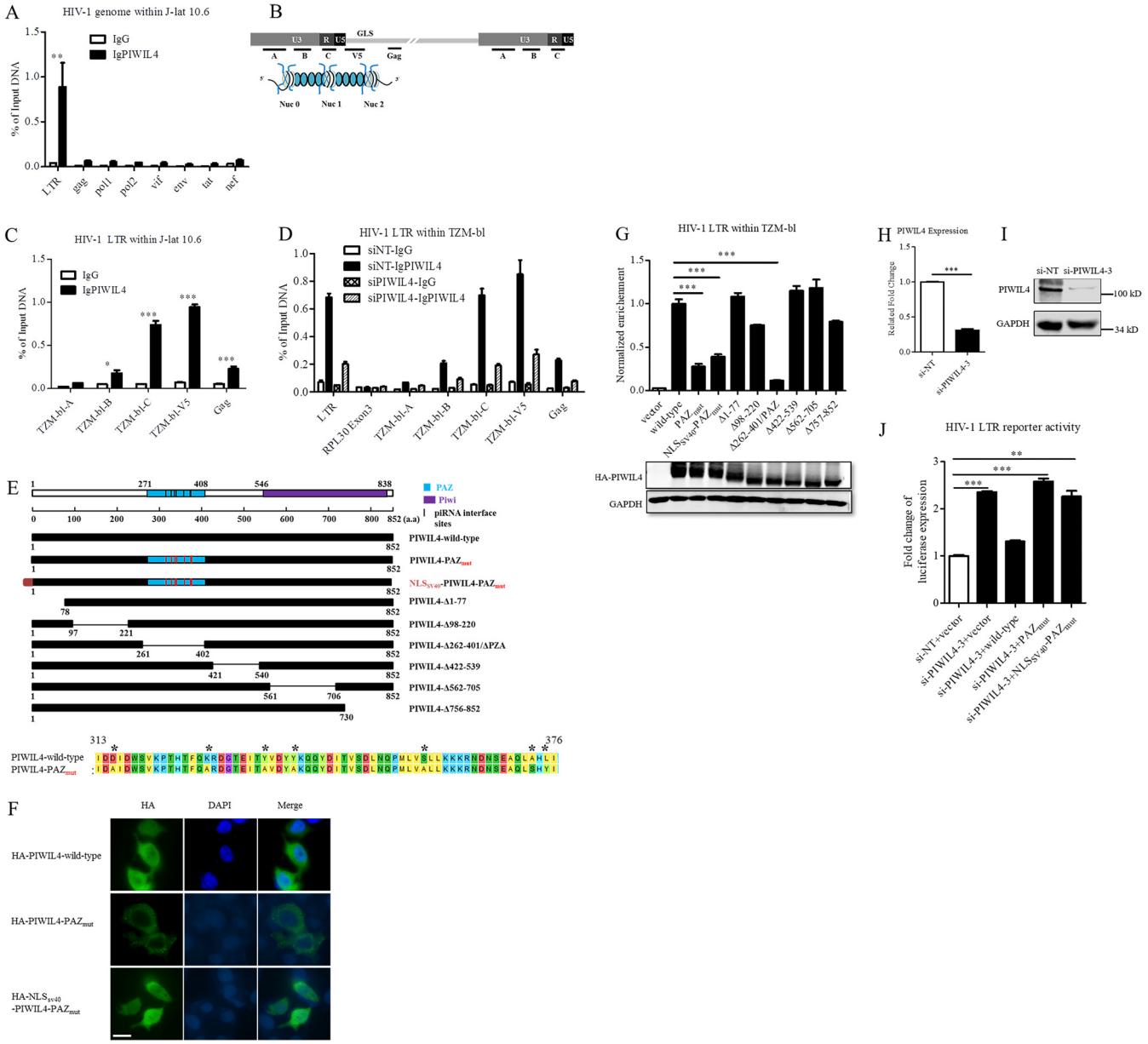

FIG 3 PAZ domain is required for PIWIL4 to be associated with the HIV-1 5′ LTR. (A) Endogenous PIWIL4 associating with HIV-1 provirus genome was analyzed by conducting ChIP-qPCR in J-lat 10.6 cells. Potential PIWIL4-associating sites separated the HIV-1 genome into 8 regions, the LTR, *gag*, *pol1*, *pol2*, *vif*, *env*, *tat*, and *nef*, which were detected using responsive primer pairs. (B) The schematic of the 5′ LTR, adjacent *gag* leader sequence (GLS), and 3′ LTR of the HIV-1 minigenome within TZM-bl cells. The HIV-1 5′ LTR has been divided into three domains: the R (repeat) region, U5, and U3. The GLS was aligned adjacent to the 5′ LTR. The positions of 3 nucleosomes, Nuc-0, Nuc-1, and Nuc-2, are indicated. The primer pairs TZM-bl-A, TZM-bl-B, TZM-bl-C, and TZM-bl-V5, as well as Gag targeting different regions, are indicated. (C) Endogenous PIWIL4 associating with the HIV-1 5′ LTR and adjacent GLS was analyzed by conducting ChIP-qPCR in J-lat 10.6 cells. Potential PIWIL4-associating sites separate the HIV-1 5′ LTR and adjacent GLS into 5 regions and were detected using responsive primer pairs as depicted in panel B. (D) Endogenous PIWIL4 associating with the HIV-1 5′ LTR and adjacent GLS was analyzed by conducting ChIP-qPCR in TZM-bl cells. Potential PIWIL4-associating sites separate the HIV-1 5′ LTR and adjacent GLS into 5 regions, which were detected using responsive primers as depicted in panel B. (E) Schematic of wild-type PIWIL4 and 8 PIWIL4 mutants. PIWIL4-PAZ$_{mut}$ was constructed with site mutations in the PAZ domain and inserted into a nuclear localization signal (NLS) from SV40 when needed. (F) Single NLS from SV40 restored nuclear entry ability of PIWIL4-PAZ$_{mut}$. HA-tagged PIWIL4-wild type, PIWIL4-PAZ$_{mut}$, and NLS$_{SV40}$-PIWIL4-PAZ$_{mut}$ were transfected separately into TZM-bl cells. Cells were fixed 48 h posttransfection, followed by immunofluorescence. Scale bar, 10 μm. (G) Endogenous PIWIL4 was knocked down by the specific siRNA targeting the 3′ UTR of the PIWIL4 transcript (si-PIWIL4-3) in TZM-bl cells, and the cells were separately transfected with wild-type PIWIL4 or 1 of 8 PIWIL4 mutants, as depicted in panel E. The expression of the wild type and all PIWIL4 mutants was confirmed by immunoblotting. ChIP-qPCR was conducted to analyze the association with the HIV-1 5′ LTR of the wild type and all PIWIL4 mutants. (H to J) Endogenous PIWIL4 was knocked down by si-PIWIL4-3 in TZM-bl cells. (H and I) The efficiency of endogenous PIWIL4 knockdown was confirmed by qRT-PCR and immunoblotting. (J) PIWIL4-depleted TZM-bl cells were restored with wild-type or mutated PIWIL4 as indicated. The luciferase activity was measured. Data represent means ± SEM from triplicates. *P* values were calculated by Student's *t* test. *, $P < 0.05$; **, $P < 0.01$; ***, $P < 0.001$.

Suv39H1, and SETDB1 (39). Repressive histone methylation and their responsive modifiers are associated with HIV-1 provirus silencing (73). To determine whether HIV-1 provirus silencing is caused by PIWIL4 introduction of repressive histone markers to the HIV-1 5′ LTR by recruiting histone modifiers, such as SETDB1 and HP1$\alpha/\beta/\gamma$, we first verified the interactions between PIWIL4 and these histone modifiers by coimmunoprecipitation (co-IP) assays in the presence of RNase A (Fig. 4A to C). Using ChIP-qPCR, we found that the knockdown of PIWIL4 decreased the amount of HP1$\alpha/\beta/\gamma$ and SETDB1 in the HIV-1 5′ LTR region in both TZM-bl and J-lat 10.6 cells (Fig. 4D and E), indicating that PIWIL4 recruited HP1$\alpha/\beta/\gamma$ and SETDB1 to the 5′ LTR. In addition, we simultaneously examined the major repressive histone modifications, including H3K9me2/3, H3K27me3, and H4K20me3, at the HIV-1 5′ LTR region and observed a decrease of H3K9me2/3, further confirming the decreased recruitment of H3K9 methylation modifiers after PIWIL4 depletion (Fig. 4F and G). Interestingly, no obvious changes in the amounts of H3K27me3 and H4K20me3 were detected (Fig. 4F). This result was consistent with those of the co-IP assays in that neither EZH2 nor SMYD2 interacted with PIWIL4 (data not shown). Meanwhile, the increased H3K4me3 at the HIV-1 5′ LTR region upon PIWIL4 depletion is in accordance with previous research that indicates that H3K4me3 is a marker of active transcription (Fig. 4F and G) (74, 75). Further, the relief of impeded initiation and elongation of transcription was consistent with the increased association of phosphorylated RNAP II (Ser-2 phosphorylation of RNAP II at the C-terminal domain) at the HIV-1 5′ LTR region after PIWIL4 depletion (Fig. 4F and G). Intriguingly, we found no change in the DNA hypermethylation signature at the two major CpG islands of the HIV-1 promoter region after PIWIL4 depletion in J-lat 8.4 cells (65 and data not shown). Contrary to J-lat 8.4 cells, the counterparts of TZM-bl and J-lat 10.6 cells both were hypomethylated. Therefore, we suggested that the promotion of PIWIL4 upon HIV-1 latency did not depend upon transcription repression induced by DNA methylation. Collectively, these results demonstrated that PIWIL4 recruited H3K9me2/3 modifiers at the HIV-1 5′ LTR region, thereby imposing histone H3K9me2/3 marks and subsequently condensing chromatin conformation to promote HIV-1 latency.

HDAC4 is recruited to the HIV-1 5′ LTR by PIWIL4. It has been shown that the nuclear PIWI/piRNA complexes take part in the chromatin modification pathway by manipulating DNA methylation and/or histone methylation around the targeted regions (49). Recently, it was reported that PIWIL2 not only stabilizes HDAC3 by competing with E3 ubiquitin ligase Siah2 but also enhances its phosphorylation via CK2a in human tumor cell lines (76). This work connects PIWI proteins with HDACs in human somatic cells. To identify and explore the interacting proteins of PIWIL4 besides DNA and histone methylation modifiers, especially those possibly involved in HIV-1 latency, we conducted an affinity purification mass spectrometry (AP-MS) assay (Fig. 5A). Among these proteins, including Ago1-3, Tudor domain-containing protein 1 (TDRD1), ATP-dependent RNA helicase A9 (DHX9), and WD repeat-containing protein 1 (WDR1), we also identified HDAC4, which has been reported to contribute to HIV-1 latency as a novel binding protein of PIWIL4 with high confidence (Fig. 5B) (12). To verify the association of HDAC4 with PIWIL4, we performed co-IP experimentation in HeLa cells transfected with either FLAG-HDAC4- or HA-PIWIL4-expressing plasmids. PIWIL4 specifically interacted with HDAC4 in the presence of RNase A, suggesting that this interaction is RNA independent (Fig. 5C and D). Accordingly, the knockdown of endogenous PIWIL4 significantly downregulated the amount of HDAC4 at the HIV-1 5′ LTR region. Due to PIWIL4 decline at the HIV-1 5′ LTR region, an increase of H3K9 acetylation was also observed (Fig. 5E and F). These results suggested that PIWIL4 recruited HDAC4 to the HIV-1 5′ LTR region and affected histone acetylation. We also observed the reactivation of HIV-1 in J-lat 10.6 cells after HDAC4 knockdown by specific shRNA to a lesser degree than that upon PIWIL4 depletion (Fig. 5G to J), which suggested that HDAC4 was partially responsible for the suppressive activity of PIWIL4 on the HIV-1 5′ LTR.

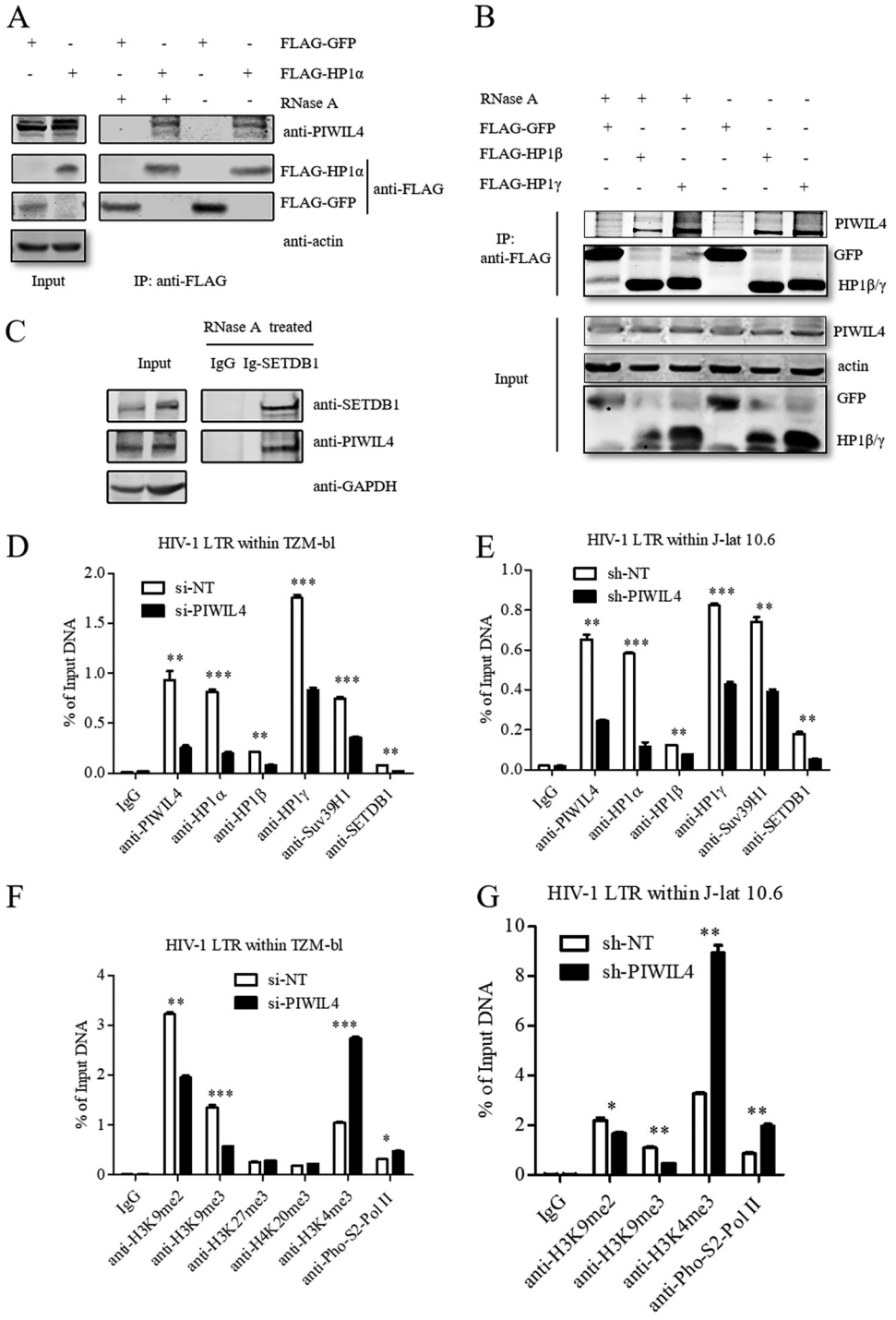

FIG 4 HIV-1 latency is enforced by PIWIL4 via its mediation of the repressive H3K9 modification on the HIV-1 5′ LTR. (A and B) HeLa cells were transfected with FLAG-HP1$\alpha/\beta/\gamma$ or FLAG-GFP. Total cell lysates were collected 48 h posttransfection for analyzing the protein interaction between FLAG-HP1$\alpha/\beta/\gamma$ and endogenous PIWIL4 by anti-FLAG immunoprecipitation and anti-PIWIL4 immunoblotting. (C) J-lat 10.6 cell lysates were analyzed for interaction between endogenous PIWIL4 and SETDB1 by anti-SETDB1 immunoprecipitation and anti-PIWIL4 immunoblotting. RNase A was added to the samples prepared for immunoprecipitation (20 μg ml^{-1}) when needed. (D and E) ChIP-qPCR assays with antibodies against PIWIL4, HP1$\alpha/\beta/\gamma$, and SETDB1 interacting with the HIV-1 5′ LTR were conducted in PIWIL4-depleted TZM-bl (D) and J-lat 10.6 cells (E). (F and G) ChIP-qPCR assays with antibodies against H3K9me2/3, H3K9ac, K3K4me3, and Pho-Ser2-Pol II were performed in PIWIL4-depleted TZM-bl (F) and J-lat 10.6 (G) cells. (F) The histone modification of H3K27me3 and H4K20me3 also was examined by ChIP-qPCR targeting HIV-1 5′ LTR in PIWIL4-depleted TZM-bl cells. Data represent means ± SEM from triplicates. *P* values were calculated by Student's *t* test. *, $P < 0.05$; **, $P < 0.01$; ***, $P < 0.001$.

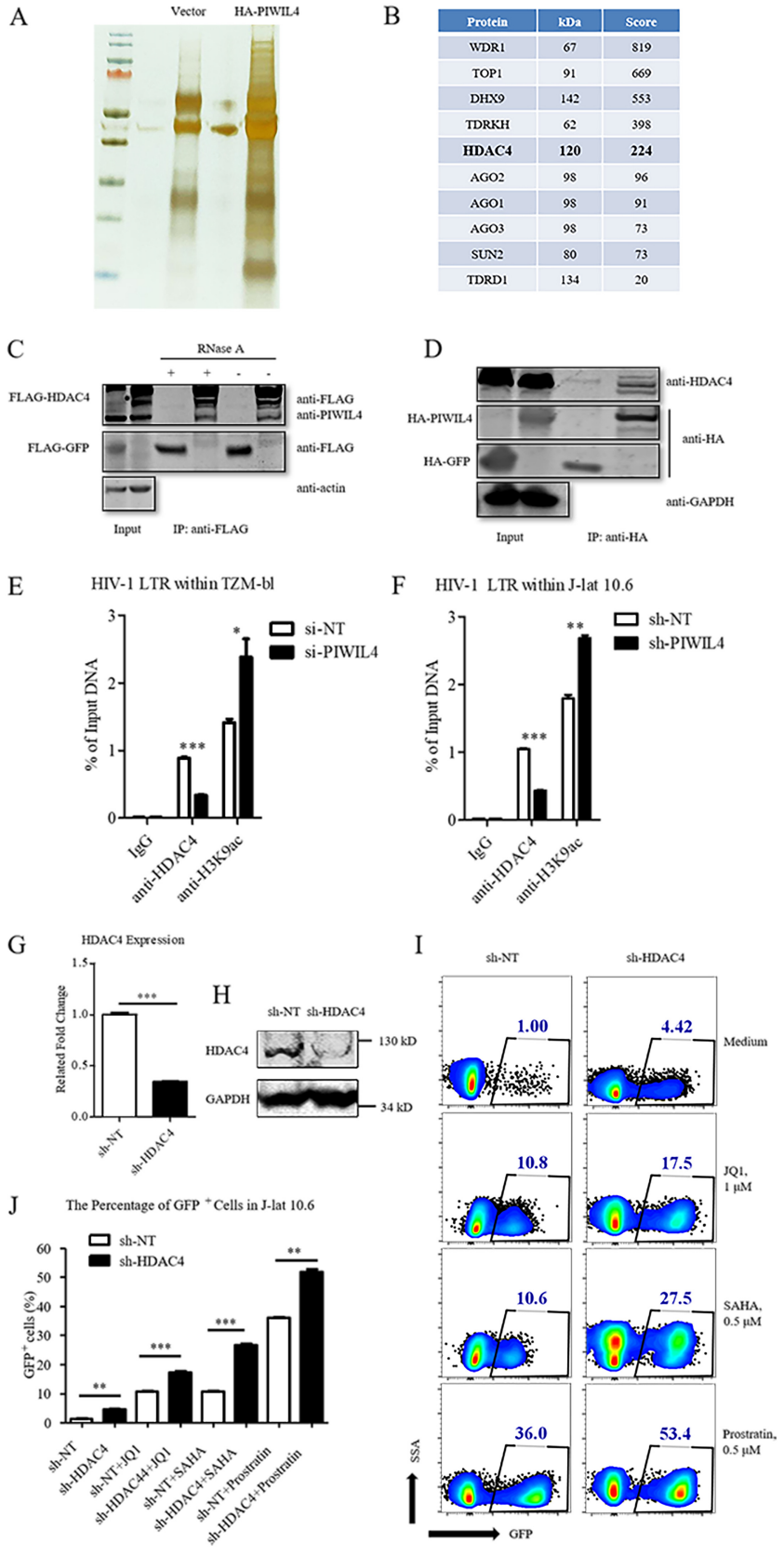

FIG 5 HDAC4 is recruited to the HIV-1 5′ LTR by PIWIL4. (A) Immunoprecipitation of host proteins associated with HA-tagged PIWIL4. J-lat 10.6 cells were transduced with lentivectors expressing HA-PIWIL4 and a puromycin resistance gene. Following puromycin treatment for a week, cells were lysed,

(Continued on next page)

Depletion of PIWIL4 promotes viral reactivation from latently infected CD4$^+$ T lymphocytes. We have determined the role of PIWIL4 in maintaining HIV-1 latency in latently infected Jurkat cells. To further validate this phenomenon in primary CD4$^+$ T lymphocytes, we modified an established method to generate a primary CD4$^+$ T lymphocyte-based latency model (64). A *bcl-2* open reading frame (ORF) with a P2A sequence at its 5′ terminus was inserted into the 3′ terminus of the *nef* ORF without its stop codon in the defective HIV-1 plasmid, pNL4-3-△E-EGFP, to express the Bcl-2 protein, which promotes cell survival in long-term culture. We knocked down PIWIL4 expression in latently HIV-1-infected human CD4$^+$ T lymphocytes from two donors by using specific siRNAs, alone or combined with SAHA treatment, to activate latent HIV-1 in these cells and then examined GFP expression (Fig. 6A and B). Compared to that of control cells, we found that HIV-1 reactivation increased 1.91 to 3.34% upon PIWIL4 depletion and 6.97 to 10.1% upon PIWIL4 depletion combined with SAHA treatment (Fig. 6C and D). These results suggested that PIWIL4 also maintains HIV-1 latency in latently infected CD4$^+$ T lymphocytes.

Depletion of PIWIL4 reactivates HIV-1 replication-competent viruses in latently infected human primary CD4$^+$ T lymphocytes. To verify whether PIWIL4 is a potential target for developing new LRAs, we analyzed the effect of PIWIL4 depletion on the reactivation of latent proviruses in primary CD4$^+$ T lymphocytes from HIV-1-infected individuals on suppressive cART for over 6 months (Table 1, patients P1 to P3). The effective depletion of PIWIL4 was confirmed at the mRNA expression level (Fig. 7A). By quantitation of intracellular (Fig. 7B) and virion-associated RNA in the supernatant, we found that PIWIL4 depletion significantly reactivated HIV-1 expression in CD4$^+$ T lymphocytes (Fig. 7C). To further evaluate whether the reactivated HIV-1 virions were replication competent, we cocultured stimulated CD4$^+$ T lymphocytes from healthy donors and PIWIL4-specific, siRNA-treated resting CD4$^+$ T lymphocytes from HIV-1-infected individuals. The accumulation of HIV-1 p24 antigen in the presence of PIWIL4-specific siRNA indicated that the reactivated virions following PIWIL4 depletion were replication competent (Fig. 7D). To investigate whether PIWIL4 depletion nonspecifically activates T lymphocytes, the expression of T cell activation surface markers, CD25 (marker for early activated T cells) and CD69 (marker for middle activated T cells), of the purified CD4$^+$ T lymphocytes were analyzed after the knockdown of PIWIL4 (Fig. 7E and F). There was no significant change in the expression of CD25 and CD69 after PIWIL4 depletion (Fig. 7G). Additionally, the CCK-8 assay determined cell viability and showed that the depletion of PIWIL4 did not suppress the viability of CD4$^+$ T lymphocytes and J-lat 8.4 cells (Fig. 7H). Altogether, these results indicated that PIWIL4 is a potential target for LRA development (77–80). Moreover, these results collectively suggested that PIWIL4 enforced HIV-1 latency in HIV-1-infected primary CD4$^+$ T lymphocytes.

DISCUSSION

HIV-1 could be strategically hidden from immunosurveillance within the cellular genome as an integrated provirus, and its activity is intrinsically and comprehensively

FIG 5 Legend (Continued)
followed by anti-HA immunoprecipitation and then SDS-PAGE, and visualized by silver staining. (B) List of partial host proteins identified as described for panel A by LC-MS/MS analysis. (C) HeLa cells were transfected with FLAG-HDAC4 or FLAG-GFP. Total cells were collected 48 h posttransfection and analyzed for protein interaction between FLAG-HDAC4 and endogenous PIWIL4 by anti-FLAG immunoprecipitation and anti-PIWIL4 immunoblotting. (D) HeLa cells were transfected with HA-PIWIL4 or HA-GFP. Total cell lysates were analyzed 48 h posttransfection for protein interaction between HA-PIWIL4 and endogenous HDAC4 by anti-HA immunoprecipitation and HDAC4 immunoblotting. RNase A was added to the samples prepared for immunoprecipitation (20 μg ml^{-1}) when needed. (E and F) ChIP assays with antibody against HDAC4 and H3K9ac were performed in PIWIL4-depleted TZM-bl (E) and J-lat 10.6 (F) cells. (G to J) The shRNA constructs were packaged into pseudotyped lentivectors and transduced into J-lat 10.6 cells for 4 days. (G and H) The efficiency of endogenous HDAC4 knockdown was confirmed by qRT-PCR and immunoblotting. (I and J) The sh-NT- and sh-HDAC4-transduced cells were treated with the indicated LRAs with shown concentrations for an additional 24 h, and HIV-1 reactivation was measured by the percentage of GFP$^+$ cells as analyzed by flow cytometry. Data represent means ± SEM from triplicates. *P* values were calculated by Student's *t* test. *, $P < 0.05$; **, $P < 0.01$; ***, $P < 0.001$.

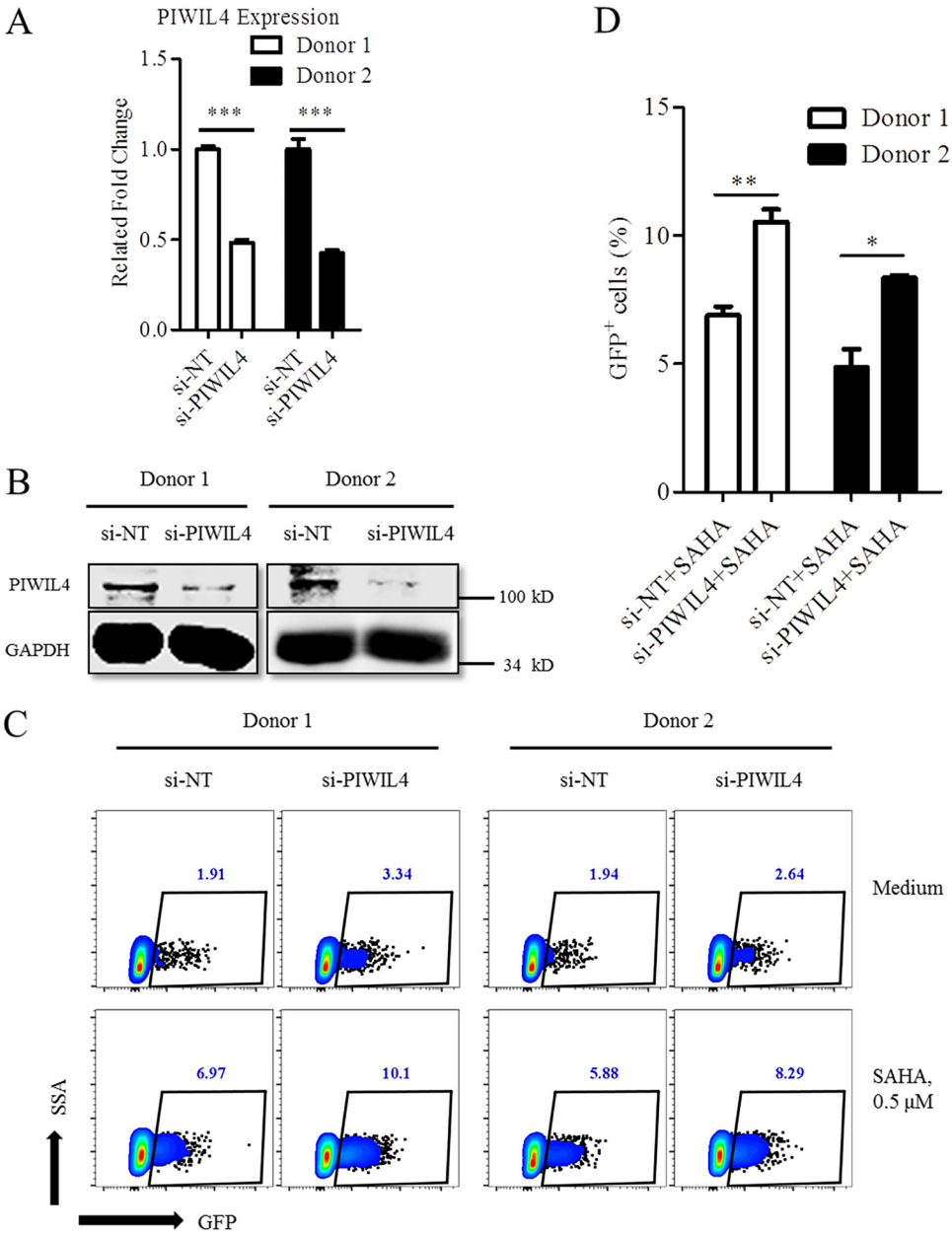

FIG 6 Depletion of PIWIL4 promotes viral reactivation from latently infected CD4$^+$ T lymphocytes. (A to D) Latently pseudotyped HIV-1-infected T lymphocytes were treated with si-PIWIL4 or si-NT for 3 days and then were analyzed by qRT-PCR and immunoblotting for the knockdown efficiency of PIWIL4 (A and B) or were treated with SAHA for an additional 2 days (C and D); viral reactivation was measured and summarized by detecting the percentage of GFP$^+$ cells. Data represent means ± SEM from triplicates. *P* values were calculated by Student's *t* test. *, $P < 0.05$; **, $P < 0.01$.

modulated by cellular and viral proteins. Among human PIWI proteins, it was first proven that PIWIL2 inhibited HIV-1 replication in activated CD4$^+$ T lymphocytes by hijacking the rare tRNA species specifically needed for HIV-1-encoded proteins; however, this protein did not appear to be involved in the maintenance of HIV-1 latency (57). Unlike PIWIL1-3, PIWIL4 manifests constitutive protein expression in both resting and activated primary CD4$^+$ T lymphocytes and J-lat cells, which suggests that PIWIL4 plays important roles in modulating gene expression in these cells.

In this study, we demonstrated that PIWIL4 enforces HIV-1 latency by suppressing HIV-1 5′ LTR-driven transcription through the recruitment of SETDB1, HP1$\alpha/\beta/\gamma$, and other repressors (e.g., HDAC4) to the HIV-1 5′ LTR. PIWIL4 binds to these repressors and

TABLE 1 Clinical characteristics of the individuals with HIV-1 infections enrolled in this study[c]

ID	Age (yr)	Sex[a]	Time since HIV-1 diagnosis (yr)	Time on cART (yr)	cART regimen[b]	Viral load (copies/ml)	$CD4^+$ count (cells/μl peripheral blood)	$CD4^+/CD8^+$ ratio
P1	26	M	3.5	2.3	TDF + 3TC + EFV	<20	473	0.79
P2	36	M	3.4	2.9	TDF + 3TC + EFV	<20	557	0.70
P3	36	F	9.0	6.0	TDF + 3TC + EFV	<20	503	0.53

[a]M, male; F, female.
[b]TDF, tenofovir disoproxil fumarate; 3TC, lamivudine; EFV, efavirenz.
[c]The clinical characteristics of the individuals with HIV-1 infections enrolled in this study were recorded on the day of sampling.

induces heterochromatin formation around the HIV-1 5′ LTR (Fig. 7I). As the results showed, the interaction between PIWIL4 and these repressors is RNA (including but not limited to piRNA) independent, which suggested that either the association of PIWIL4 with piRNA or the RNA as an adaptor or bridge is not required for the interaction between PIWIL4 and HP1$\alpha/\beta/\gamma$. The knockdown of PIWIL4 induced reactivation of HIV-1 in latently HIV-1-infected Jurkat T cells and primary $CD4^+$ T lymphocytes and in resting $CD4^+$ T lymphocytes from HIV-1-infected individuals on suppressive cART. HIV-1 latency is systematically modulated by host factors and viral proteins, and we believed that HIV-1 latency would be reactivated to a large extent when simultaneously targeting and depleting different factors involved in HIV-1 latency. In the absence of PIWIL4, latently HIV-1-infected Jurkat T cells were more sensitive to reactivation with known LRAs, such as SAHA, JQ1, and prostratin. As shown in Fig. 2C, when we individually treated J-lat 10.6 cells with SAHA, JQ1, and prostratin, the proportion of activated GFP^+ cells was 14.1%, 18.2%, and 25.7%, respectively. In the presence of PIWIL4 (9.93% for PIWIL4 depletion alone), the responsive activated proportion for SAHA, JQ1, and prostratin was up to 39.9%, 57.4%, and 74.9%, respectively (Fig. 2C and E), which were significantly higher than levels for those treated with individual LRAs alone. A similar phenomenon also was observed within J-lat 8.4 cells (Fig. 2D and F). Moreover, similar results were found when we knocked down PIWIL4 in TZM-bl cells in the absence or presence of TNF-α treatment. The activated effect of PIWIL4 depletion alone on LTR basal activity was up from 2.4- to 3.5-fold upon TNF-α treatment compared to levels for their control cells (Fig. 1H). We have also proved that PIWIL4 depletion was irrelevant to the NF-κB signal pathway (Fig. 1I), which is the major target of TNF-α and prostratin treatment. SAHA was reported to repress the activity of all human class I and II histone deacetylases (HDACs) to various degrees (81). Thus, SAHA treatment could significantly enhance histone acetylation, while prostratin or TNF-α treatment activates the NF-κB pathway and JQ1 treatment antagonizes BRD4's competitive inhibition of the recruitment of p-TEFb by Tat (68). According to our results, PIWIL4 depletion induced an obvious decline of H3K9me2/3 and a slight increase of H3K9ac around the HIV-1 promoter region. Taken together, these results suggested that the hyperacetylation caused by SAHA treatment and the hypomethylation caused by PIWIL4 depletion worked together to loosen the chromatin conformation, or PIWIL4 depletion worked together with other stimuli to facilitate HIV-1 5′ LTR transcription activity. Thus, our study reveals a previously unknown role of PIWIL4 in the HIV-1 life cycle, which likely occurs through PIWIL4 reinforcement of HIV-1 latency in HIV-1 latently infected cells. The knockdown of PIWIL4 significantly enhanced HIV-1 reactivation upon stimulation with SAHA, JQ1, or prostratin.

Although the interaction between PIWIL4 and the above-mentioned repressors occurred in an RNA-independent manner, the association of piRNAs with the conserved PAZ domain of PIWIL4 was required for PIWIL4 to be associated with the HIV-1 5′ LTR and to suppress HIV-1 5′ LTR-driven transcription in the present study, which was consistent with a previous report (49). The PIWIL4 ChIP-qPCR assays indicated that PIWIL4 associates with the HIV-1 5′ LTR between Nuc-1 and Nuc-2. For future research, it will be important to search for the potential complementary pairing between piRNAs or piRNA-like molecules and their recognized DNA or nascent mRNAs transcribed from these loci.

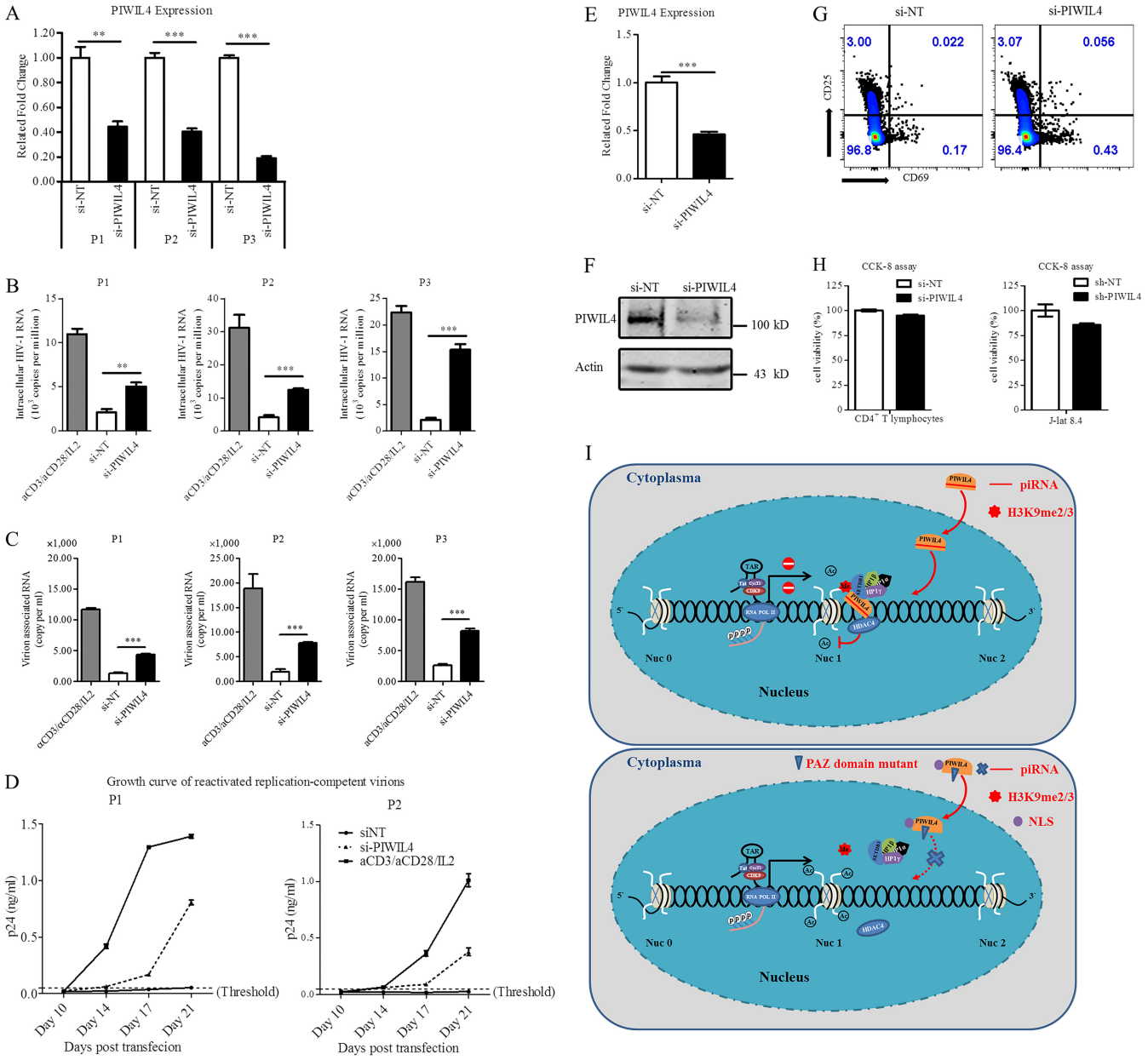

FIG 7 Depletion of PIWIL4 reactivates HIV-1 replication-competent viruses in latently infected human primary CD4$^+$ T lymphocytes. (A to C) The endogenous PIWIL4 in primary resting CD4$^+$ T lymphocytes from HIV-1-infected individuals on suppressive cART for more than 6 months. (A) Cells were knocked down by si-PIWIL4 or treated with si-NT, and the expression of PIWIL4 was checked by qRT-PCR. (B and C) Three days posttransfection, intracellular HIV-1 RNA and virion RNA in the supernatant were isolated and quantitated by qRT-PCR. Cells stimulated with aCD3/aCD28 antibodies/IL-2 for 3 days were used as a positive control. (D) Resting CD4$^+$ T lymphocytes from HIV-1-infected individuals were isolated and transfected with si-PIWIL4 or si-NT or were stimulated with anti-CD3/CD28 antibodies. Three days posttransfection, stimulated CD4$^+$ T lymphocytes from healthy donors were washed, collected, and cocultured with PIWIL4-specific siRNA-treated resting CD4$^+$ T lymphocytes from HIV-1-infected individuals for another 18 days. The medium was half-refreshed with complete medium supplemented with IL-2 every 2 to 3 days. Stimulated CD4$^+$ T lymphocytes from healthy donors were added into each group of virus cultures, as indicated, on days 10 and 17 posttransfection. The supernatants were separately collected on day 10, day 14, day 17, and day 21 posttransfection and stored at −80°C until the endpoint of the assays and were uniformly measured with ELISA. Dashed lines indicated the limit of detection (L.O.D.) of 50 pg/ml of p24. Results from triplicates are represented by means ± SEM. **, $P < 0.01$; ***, $P < 0.001$. (E to G) Resting CD4$^+$ T lymphocytes from healthy donors transfected with si-PIWIL4 or si-NT. (E and F) Cells were collected after 48 h, and PWII4 expression was determined by qRT-PCR and immunoblotting. (G) The expression of T cell activation markers CD25 and CD69 in the isolated CD4$^+$ T lymphocytes from healthy donors was analyzed by flow cytometry 3 days posttransfection of si-NT or si-PIWIL4. (H) Depletion of PIWIL4 did not suppress the viability of CD4$^+$ T lymphocytes and J-lat 8.4 cells. After depletion of PIWIL4, cell viability of CD4$^+$ T lymphocytes and J-lat 8.4 cells by CCK-8 assay were assessed. (I) Schematic of PIWIL4-enforced HIV-1 latency. Data represent means ± SEM from triplicates. *P* values were calculated by Student's *t* test. **, $P < 0.01$; ***, $P < 0.001$.

Through the development and utilization of high-throughput sequencing technologies, a class of small noncoding RNAs was derived from tRNA and consequently termed tRNA-derived fragments (tRFs). tRFs are involved in modulating principle cellular functions under physiological or pathological conditions (82–86). Additionally, in monocyte/dendritic cells, PIWIL4 suppressed CD1a expression associated with td-piR(Glu), which is processed from tRNA-Glu (39). tRNA-3, a major type of tRF, is enriched in $CD4^+$ T lymphocytes and is involved in the reverse transcription of human T-cell leukemia virus type 1 (HTLV-1) (87). As PIWIL4 is associated with tRFs in somatic cells, it is possible that PIWIL4 utilizes tRFs to recognize the HIV-1 5′ LTR (38, 39). Unfortunately, we did not find any functional piRNAs on the HIV-1 5′ LTR region (data not shown). As PIWIL4 suppresses HIV-1 5′ LTR-driven transcription in different cell lines and primary $CD4^+$ T lymphocytes, it is reasonable to assume that the piRNA species relevant to HIV-1 latency originate from housekeeping genes or ubiquitously expressed genes.

The 18 characterized HDACs in humans can be grouped into four major classes: classes I to IV. HDAC4 belongs to the subclass IIa, accompanied by HDAC-5, -7, and -9 (88). HDAC1 to -4 all were reported to play important roles in contributing to HIV-1 latency (10–14). HDAC4 functions in histone or nonhistone protein deacetylation via recruitment of NCoR/silencing mediator of retinoid and thyroid hormone receptor (SMRT) complexes (89, 90). The consequent hypoacetylation of histones favors the formation of heterochromatin (21). In addition, HDAC4 has been reported to be involved in histone methylation (91). Our results indicated that HDAC4 can be recruited to the HIV-1 5′ LTR region to induce hypoacetylation of histones in a manner similar to that of the modifiers of H3K9 methylation. The hypoacetylation and hypermethylation of histones simultaneously regulated by PIIWL4 synergistically maintained HIV-1 latency.

Besides HDAC4, SUN2, a newly identified modulator of HIV-1 latency, is also an interesting candidate for potential interaction with PIWIL4. The mechanism by which SUN2 modulates HIV-1 latency appears to be irrelevant to the manipulation of epigenetic modification around the HIV-1 5′ LTR region (22). Indeed, SUN2 could interact with lamin A/C and impede the initiation and elongation of HIV-1 translation by enforcing repressive chromatin conformation (22). It was reported that histone modifications play important roles in the regulation of the structural and biological functions of chromatin, which seem to be irrelevant to lamins (92, 93). Therefore, the undetermined cross-talk between PIWIL4 and SUN2 in modulating the chromatin conformation around the HIV-1 5′ LTR is worthy of further study.

In conclusion, our study demonstrates that PIWIL4, most likely being bound with piRNA, is associated with the HIV-1 5′ LTR. It not only imposes repressive H3K9me2/3 marks by recruiting the responsive methyltransferase SETDB1 and HP1$\alpha/\beta/\gamma$ but also promotes the tethering of the suppressive factor HDAC4 to the 5′ LTR, which together facilitate the formation and maintenance of the condensed chromatin conformation state around the HIV-1 5′ LTR region. These results shed light upon the connection between nuclear PIWIL4 and HIV-1 latency and propose a prospective target for future therapeutic strategies.

MATERIALS AND METHODS

Ethics statement. The HIV-1-infected participants who had undergone combined antiretroviral therapy with undetectable HIV-1 viral loads in plasma (fewer than 50 copies/ml) and high $CD4^+$ T cell count (at least 350 μl^{-1}) for a minimum of 6 months were recruited for our study by the Department of Infectious Diseases in Guangzhou 8th People's Hospital, Guangzhou, China. Approval of the research was signed by the Ethics Review Board of Sun Yat-Sen University and Guangzhou 8th People's Hospital. All participants provided written informed consent.

Cell culture. Blood samples from healthy donors were acquired from the Blood Center of Guangzhou, China. Human peripheral blood mononuclear cells (PBMCs) were isolated through Ficoll gradient centrifugation. Human primary $CD4^+$ T lymphocytes were further purified with a human $CD4^+$ T cell isolation kit according to the manufacturer's instructions (BD Biosciences). PBMCs or primary $CD4^+$ T cells were cultured in RPMI 1640 supplemented with 10% fetal bovine serum (FBS) (ThermoFisher), 1% penicillin-streptomycin (ThermoFisher), and 1% L-glutamine (ThermoFisher). $CD4^+$ T cells were stimulated with anti-CD3 antibody (1 μg ml^{-1}; BD Biosciences), anti-CD28 antibody (1 μg ml^{-1}; BD Biosci-

ences), and interleukin-2 (IL-2; 10 ng ml^{-1}; R&D Systems) for 3 days, followed by washing three times with phosphate-buffered saline (PBS) and keeping the culture in the presence of IL-2 (10 ng ml^{-1}) until the endpoint of the experiments. The activation status of cells was monitored by detecting the expression of CD25 and CD69. Allophycocyanin (APC)–cyanine 7 (Cy7)–anti-CD25 (M-A251; BD Biosciences)- and phycoerythrin–Cy7–anti-CD69 (FN50; eBioscience)-specific antibodies were used for immunostaining. Cells were detected by BD LSRFortessa flow cytometry (BD Biosciences) and analyzed by FlowJo V10 (Tree Star). J-lat 8.4 and 10.6 cell lines, which were created by Eric Verdin and his colleagues (65), were kind gifts from the laboratory of Robert F. Siliciano (Department of Medicine, Johns Hopkins University School of Medicine, Baltimore, MD, USA). The two J-lat cell lines were cultured in RPMI 1640 supplemented with 10% FBS, 1% penicillin-streptomycin, and 1% L-glutamine. The human embryonic kidney cell line HEK293T (CVCL_0063; ATCC), HeLa cells (CVCL_0030; ATCC), and TZM-bl cells (8129) harboring an HIV-1 promoter-driven luciferase gene, which were obtained from the NIH AIDS Reference Reagent Program, were maintained in Dulbecco' modified Eagle's medium (DMEM) (ThermoFisher) supplemented with 10% FBS, 1% penicillin-streptomycin, and 1% L-glutamine. All cells had been tested and confirmed to be mycoplasma free by PCR assays. All cells were maintained in a clean incubator at 37°C and 5% CO_2.

siRNA transfection and luciferase reporter assays. Two siRNAs targeting CDS (si-PIWIL4-1, 5′ GGA CGG AAC TTC TAT AATC 3′; si-PIWIL4-2, 5′ GGA CAA TCC AAG AAG AAAT 3′) and one siRNA targeting the 3′ UTR (si-PIWIL4-3, 5′ GAT GAC AGA TAA ACA GAGT 3′) of the PIWIL4 transcript, as well as nontarget control siRNA (si-NT), were purchased from RiboBio (Guangzhou, China). TZM-bl or HeLa cells were seeded in a 48-well cell culture plate. After 12 h, transfection was performed using Lipofectamine RNAiMAX (ThermoFisher) for siRNA or Lipofectamine 2000 for plasmid expressing HIV-1 Tat alone in TZM-bl or together with HIV-1 promoter reporter plasmid in HeLa cells according to the manufacturers' instructions. Each siRNA was used for at least three biological replicates. Twenty-four hours posttransfection, cells were further treated with TNF-α (50 ng/ml) for an additional 24 h when needed. Cells were washed with PBS and split with passive lysis buffer (Promega). Luciferase in the cell lysates was measured with a luciferase reporter assay system (Promega). Fold changes were normalized by comparison to levels for si-NT according to light units. siRNAs were transfected into resting $CD4^+$ T lymphocytes from healthy donors or HIV-1-infected individuals on cART as follows. Without prior activation, resting $CD4^+$ T lymphocytes as the negative control or PIWIL4 depletion groups were transfected with the respective siRNAs by Lipofectamine RNAiMAX (ThermoFisher) according to the manufacturer's suggestions, with some modifications according to a previous report from our laboratory (64). Briefly, 1×10^6 ml^{-1} to 2×10^6 ml^{-1} cells were transfected with 200 pmol PIWIL4-specific or nontargeting siRNAs together with 10 μl Lipofectamine RNAiMAX (ThermoFisher). Either the siRNAs or RNAiMAX was preincubated with 150 μl Opti-MEM I medium without serum (ThermoFisher), mixed gently and thoroughly, and kept incubated for 10 to 15 min at room temperature in each well of a 24-well culture plate. To each well containing RNAi duplex-Lipofectamine RNAiMAX complexes, we added 1 ml of the diluted resting $CD4^+$ T lymphocytes. We incubated the cells for half a day at 37°C in a CO_2 incubator, washed the cells with PBS, and kept the cultured cells in the conditional RPMI 1640 medium with 10% FBS for further assays.

Plasmids and shRNAs. The cDNA coding sequence regions of PIWIL4, HDAC4, and HP1$\alpha/\beta/\gamma$ tagged with N-terminal hemagglutinin (HA) or FLAG were amplified by reverse transcription-PCR (RT-PCR), with the mRNA of human $CD4^+$ T lymphocytes as the template. They then were subcloned into pcDNA3.1-intron vector. PIWIL4-PAZ_{mut} and six sequential truncated PIWIL4 mutants were constructed from pcDNA3.1-intron-HA-PIWIL4 by overlapping PCR. The nuclear localization signal (NLS) from simian virus 40 (SV40) was inserted between the HA tag and CDS of PIWIL4 for PIWIL4-PAZ_{mut} when needed. pGL3-LTR-luc with or without two consecutive mutated NF-κB binding sites (64) and psi-check-2-3′ LTR were constructed by PCR amplification of the corresponding DNA fragment from pNL4-3 and then inserted into the pGL3-basic and psi-check-2 vectors (Promega, Madison, WI), respectively. The *P2A-bcl-2* gene was chemically synthesized and inserted into the end of the *nef* region of the pNL4-3-ΔE-EGFP proviral plasmid. The accuracy of all clones was confirmed by DNA sequencing. shRNA targeting luciferase (5′ ACC GCC TGA AGT CTC TGA TTAA 3′) was set as nontargeting control (sh-NT) (94). The two shRNAs targeting sequences against PIWIL4 were used in combination (5′ GCT GCA TTT GTT AGA GCT ATA 3′; 5′ CCG ACC ATA TGC AGA GAC TTA 3′) (Sigma-Aldrich), and the two shRNAs targeting sequences against HDAC4 were used in combination (5′ GGT TTA TTC TGA TTG AGA ATT 3′; 5′ GAA TCT GAA CCA CTG CAT TTC 3′) (95, 96). Target sequences were subcloned into the pLKO.1-RFP shRNA expression vector, which was derived from pLKO.1-puro. The puromycin resistance gene was replaced by the red fluorescent protein (RFP) tag. Calcium phosphate-mediated transfection of HEK293T cells was performed to produce the pseudotyped viral stocks of shRNA lentiviruses as previously described (97). Vesicular stomatitis virus glycoprotein (VSV-G) expression vector and psPAX2 were obtained from Addgene (Addgene plasmid numbers 12259 and 12260). The infection of J-lat 8.4 and 10.6 cells with the concentrated shRNA lentiviruses was performed as previously described (19). Ninety-six hours postinfection, the cells were treated with SAHA (0.5 μM; Selleckchem), (+)-JQ1 (1 μM; Selleckchem), or prostrain (0.5 μM; Sigma-Aldrich) for another 24 h. J-lat 8.4 infected with PIWIL4-specific shRNA (sh-PIWIL4) or sh-NT was treated with decitabine (5 μM; Selleckchem) for 24 h. The medium then was refreshed and the cells were cultured for an additional 3 days as previously described, with some modifications (65). The reactivation of J-lat 8.4 and 10.6 cells was determined as previously described (19).

HIV-1 infection. HEK293T cells at 3×10^6 cells were plated on 10-mm cell culture dishes. Twenty-four hours later, calcium phosphate-mediated transfection was conducted to generate replication-competent HIV-1/NL4-3 virus-like particles. Cell supernatants were harvested at 48 h posttransfection and were stored at −80°C. As previously described (64), the activated primary $CD4^+$ T lymphocytes were

seeded into 24-well cell culture plates (1×10^6 ml^{-1} to 2×10^6 ml^{-1}, 1 ml per well) and were transfected with 200 pmol PIWIL4-specific or nontargeting siRNAs with Lipofectamine RNAiMAX (ThermoFisher) according to the manufacturer's instructions. Eight to twelve hours later, the cells were infected by HIV-1/NL4-3 with the equivalent of 10 ng HIV-1 p24 antigen per well at 37°C. Three hours postinfection, the cells were washed with PBS 3 times and cultured in the conditional RMPI 1640 medium with IL-2 (10 ng ml^{-1}) supplementation. The culture supernatants were collected at 12 h (day 0), day 3, day 6, and day 9 postinfection. All of the supernatants were detected using the HIV-1 p24 enzyme-linked immunosorbent assay (ELISA) kit according to the manufacturer's instructions (Clontech).

Antibodies. The following antibodies were used for ChIP, co-IP, or immunoblotting: normal rabbit anti-IgG antibody (2729; CST), anti-PIWIL4 antibody (ab180867; Abcam), anti-HP1α antibody (ab77256; Abcam), anti-HP1β antibody (10241-2-AP; Proteintech), anti-HP1γ antibody (11650-2-AP; Proteintech), anti-SETDB1 antibody (11231-1-AP; Proteintech), anti-HDAC4 antibody (32035; SAB), anti-H3K4me3 antibody (ab8580; Abcam), anti-H3K9me2 antibody (A2359; ABclonal), anti-H3K9me3 antibody (ab8898; Abcam), anti-H3K27me3 antibody (A2363; ABclonal), anti-H4K20me3 antibody (ab9053; Abcam), anti-H3K9-acetyl antibody (9649; CST), anti-Pho-S2-Pol II antibody (ab5095; Abcam), anti-HA antibody for ChIP (C29F4; CST), normal rabbit anti-IgG antibody (2729; CST) and anti-PIWIL4 antibody (38601; SAB) for co-IP, anti-HA antibody for immunoblotting and immunofluorescence (M180-3; MBL), and anti-DDDDK antibody (PM020; MBL), anti-glyceraldehyde-3-phosphate dehydrogenase (GAPDH) antibody (10494-1-AP; Proteintech), anti-actin antibody (60008-1-Ig; Proteintech), IRDye 680RD goat anti-mouse IgG antibody (926-68070; LI-COR Biosciences), IRDye 800CW goat anti-rabbit IgG antibody (926-32211; LI-COR Biosciences), and goat anti-mouse IgG H&L (Alexa Fluor 488) (ab150113) for immunoblotting.

Real-time RT-PCR. Total cellular RNA or supernatant virion RNA was extracted using TRIzol reagent (ThermoFisher) and reverse transcribed into cDNA with a PrimeScript RT reagent kit (TaKaRa). Real-time PCR was conducted using SYBR EX-taq premix (TaKaRa) in a CFX96 real-time PCR detection instrument (Bio-Rad). The data were analyzed by a SYBR green-based system (Bio-Rad), semiquantified, and normalized to GAPDH or quantified with the help of a standard curve. Primer pairs were the following: *GAPDH*, forward, 5′ ATC CCA TCA CCA TCT TCC AGG 3′; reverse, 5′ CCT TCT CCA TGG TGG TGA AGA C 3′; *PIWIL1*, forward, 5′ GAC TGG GGT TTG AGC TTT GAT TCC 3′; reverse, 5′ TTA TTG CTT TTC TCA TTT GCA TGC C 3′; *PIWIL2*, forward, 5′ ATC CTT TCC GAC CAT CGT TC 3′; reverse, 5′ GTC CTT GCG TAC CAG ATT AGC 3′; *PIWIL3*, forward, 5′ TAC AGT GGT ACA GCT ACT CGC CAA C 3′; reverse, 5′ CGA CGT GGG CGT GAG TTC T 3′; and *PIWIL4*, forward, 5′ AAT GCT CGC TTT GAA CTA GAG AC 3′; reverse, 5′ ATT TTG GGG TAG TCC ACA TTA AAT C 3′ (47). For the quantification of HIV-1 reactivation in primary CD4$^+$ T lymphocytes of HIV-1-infected individuals on suppressive cART, a specific reverse primer was used for reverse transcription of HIV-1 RNA: 5′ GCT TCA GCA AGC CGA GTC CTG CGT C 3′. The number of copies of reverse-transcribed HIV-1 cDNA per million CD4$^+$ T lymphocytes or per microliter of supernatant was calculated and quantified, as previously described, with the following primer pairs: HIVTotRNA, forward, 5′ CTG GCT AAC TAG GGA ACC CAC TGC T 3′; reverse, 5′ GCT TCA GCA AGC CGA GTC CTG CGT C 3′. After quantitation, an *in vitro*-transcribed HIV-1 RNA was used as the external control for measuring HIV-1 RNAs. The threshold cycle of each group was converted to mass and further converted to copies. The final expression of intracellular or virion-associated HIV-1 RNA was represented as 10^3 copies of viral RNA per million CD4$^+$ T cells or per microliter of supernatant, respectively, as previously described (64, 98).

ChIP-qPCR. ChIP experiments were conducted according to the manufacturer's instructions (CST). Briefly, approximately 4×10^6 TZM-bl or 8×10^6 J-lat 10.6 cells were prepared for a single immunoprecipitation (IP) assay. TZM-bl cells were transfected with wild-type, mutated, or truncated PIWIL4 when needed. In the presence or absence of transfected PIWIL4, TZM-bl or J-lat 10.6 cells were cross-linked with 1% formaldehyde (Sigma-Aldrich) for 10 min and quenched with 0.125 M glycine for another 5 min at room temperature. After lysis, nuclear pellets from IP preparations were washed, centrifuged, resuspended, and digested with 0.5 μl micrococcal nuclease in 100 μl buffer B supplemented with dithiothreitol at 37°C for 20 min. The samples were inverted three times every 4 min. The digestion was terminated by adding 50 mM EDTA, followed by centrifugation at 13,000 rpm for 1 min at 4°C. The suspension of the nuclear pellet with ChIP buffer was further processed by sonication for 1 min (20 s on, 30 s off) at 40% amplitude. After centrifugation (10,000 rpm for 10 min at 4°C), the supernatants were transferred into new tubes and stored at −80°C or directly used for downstream experiments. The concentration and fragment length of the sheared chromatin DNA were analyzed by measuring the optical density at 260 nm (OD_{260}) and by electrophoresis on a 1% agarose gel, respectively. In general, the size range should be between 150 and 900 bp in length.

Approximately 10 μg chromatin DNA was used for each IP experiment in 500 μl ChIP buffer, in which 2% of the chromatin DNA was used as the input sample to calculate the enrichment efficiency. Chromatin DNA was incubated with the indicated antibodies at 4°C overnight with rotating. Thirty microliters of ChIP-grade protein G magnetic bead slurry (CST) was added to each sample at 4°C for another 2 h. Each IP sample was washed 3 times with low-salt and 1 time with high-salt washing buffers. The input and immunoprecipitated DNA were further processed with a series of steps of reverse cross-linking and protein digestion with proteinase K, purified, and analyzed by real-time PCR. The primer pairs targeting the HIV-1 genome within J-lat 10.6 cells and the HIV-1 5′ LTR, and its proximal region within TZM-bl cells, were used as previously described (19, 20).

Gel-LC-MS/MS analysis. The HA-tagged PIWIL4 protein was stably overexpressed in J-lat 10.6 cells after puromycin selection one week after transduction by the modified pHIV-puro lentiviral vector. pHIV-puro was reconstructed from pHIV-EGFP (Addgene plasmid 21373), as the enhanced GFP (EGFP) gene was replaced by a puromycin resistance gene. The control and HA-tagged PIWIL4 cell samples were processed by identical affinity purification procedures, separated through 10 to 20% SDS-PAGE (Ther-

moFisher Scientific), and then visualized with the ProteoSilver Plus silver stain kit (Sigma-Aldrich) according to the manufacturer's instructions. The entire gel was cut to pieces of suitable size, followed by in-gel digestion with trypsin. All digestates were processed sequentially by liquid chromatography-tandem mass spectrometry (LC-MS/MS) to characterize the coimmunoprecipitated host proteins within these gel slices as described previously (99).

Coimmunoprecipitation and immunoblotting. HeLa cells transfected with HA-tagged or FLAG-tagged protein expression vectors were lysed with NP-40 lysis buffer (10 mM Tris-HCl, pH 7.4, 150 mM NaCl, 0.5% NP-40, 1% Triton X-100, 10% glycerol, 2 mM EDTA, 1 mM Na_3VO_4, and 1% protease inhibitor cocktail [Sigma-Aldrich]) for 30 to 60 min on ice with brief vortexing every 10 min. After centrifugation for 10 min at 12,000 $\times$ *g*, the lysates were incubated with the anti-HA-tag beads, anti-FLAG-tag beads (Sigma-Aldrich), or anti-SETDB1 antibody overnight at 4°C while rotating. RNase A was added to the incubated samples (20 μg ml^{-1}) when needed. The immunoprecipitates were washed, eluted by boiling in SDS loading buffer, and separated by SDS-PAGE for further immunoblotting with the indicated antibodies. For immunoblotting, TZM-bl cells were cotransfected with the plasmids of wild-type, mutated, or truncated PIWIL4 and siRNA targeting the 3′ UTR of the PIWIL4 transcript. Alternatively, HeLa cells were transfected with PIWIL4-specific or nontarget siRNAs. At 48 h posttransfection, cells were collected and disrupted with ice-cold NP-40 lysis buffer for 30 to 60 min. The cell lysates were clarified with centrifugation, boiled in reducing SDS loading buffer, and analyzed by SDS-PAGE. For immunoblotting, 10% of total lysates was used as the input for the co-IP assays, and GAPDH (10494-1-AP; Proteintech) or actin (60008-1-Ig) was used as the loading control. The secondary antibodies were 680RD goat anti-mouse IgG antibody (926–68070; LI-COR Biosciences) and 800CW goat anti-rabbit IgG antibody (926–32211; LI-COR Biosciences). Images were acquired with an Odyssey CLX imager (LI-COR Biosciences) and analyzed by Image Studio Lite, v.4.0.

Immunofluorescence assays. TZM-bl cells were seeded on chambered coverglass (ThermoFisher) and transfected as indicated. After 48 h posttransfection, cells were washed three times with PBS and fixed with 4% paraformaldehyde at room temperature for 10 min. The cells were washed three times with PBS and blocked with PBS containing 0.5% bovine serum albumin (BSA) at room temperature for half an hour. Cells then were incubated with anti-HA primary antibody (M180-3; MBL) at 4°C overnight. Following washing with 0.1% Tween 20-PBS (PBS-T) 3 times, the cells were incubated with goat anti-mouse IgG H&L (Alexa Fluor 488) (ab150113; Abcam) at room temperature for an hour. Cells then were washed with 0.1% PBS-T three times and incubated with 4′,6-diamidino-2-phenylindole (DAPI) at room temperature for 5 min, after which the cells were washed with 0.1% PBS-T 3 times. Images were acquired by DMI6000B/DFC360FX confocal microscopy (Leica).

HIV-1 *in vitro* latency model. The HIV-1 primary latency model was constructed as previously described, with some modifications (64). Briefly, the pseudotyped HIV-1/VSV-G virus was packaged in HEK293T cells by cotransfecting pNL4-3-ΔE-EGFP-Nef-P2A-Bcl-2 and pVSV-G. The activated primary CD4$^+$ T lymphocytes from healthy individuals were infected with this pseudotyped virus, and the GFP-positive cells were sorted by fluorescence-activated cell sorting (FACS), using BD FACSAria II flow cytometry (BD Biosciences) 4 days postinfection, and recovered by culturing in conditioned RPMI 1640 medium containing IL-2 (10 ng ml^{-1}; R&D Systems) for 3 days. These cells were cultured for ~3 weeks with a low concentration of IL-2 (2 ng ml^{-1}; R&D Systems), and then the cells were subjected to activation by various reagents, as indicated in Fig. 6.

CCK-8 assays. Cell counting kit-8 (CCK8) was used to detect the viability of CD4$^+$ T lymphocytes and J-lat 8.4 cells upon PIWIL4 depletion. Cells (2 $\times$ 10^4/well) and CCK-8 reagents (10 μl/well) were premixed and added into the 96-well plates. After incubation at 37°C with 5% CO_2 for 4 h, the absorbance at 450 nm was detected by using the GloMax Discover system (GM3000; Promega).

Virus outgrowth assays. The virus outgrowth assay was conducted as previously described, with some modifications (100). Briefly, resting CD4$^+$ T lymphocytes were isolated from HIV-1-infected individuals who were on suppressive cART for at least 6 months. These CD4$^+$ T lymphocytes were transfected with siRNAs targeting PIWIL4 or the nontarget control for 8 h or were activated with aCD3/aCD28 antibodies for 3 days. For the siRNA transfection, primary CD4$^+$ T lymphocytes (1 $\times$ 10^6 ml^{-1}, 1 ml per well of 24-well cell culture plates) were transfected with 200 pmol the respective siRNAs by Lipofectamine RNAiMAX (ThermoFisher) without prior activation according to the manufacturer's suggestions, with some modifications. All cells then were cultured in the conditioned RPMI 1640 medium with 10% FBS (ThermoFisher) in the presence of recombinant IL-2 (RD Systems). Seventy-two hours posttransfection, all cells were supplemented with activated CD4$^+$ T lymphocytes from healthy donors. The supernatants were collected and half-refreshed with complete medium supplemented with IL-2 every 2 to 3 days. On day 3 posttransfection, the suspensions of stimulated CD4$^+$ T lymphocytes from healthy donors were mixed with the CD4$^+$ T lymphocytes from HIV-1-infected individuals on day 10 and day 17 posttransfection. All of the supernatants separately collected were stored at −80°C until the endpoint of the assays and were uniformly measured for the released viral antigen with the HIV-1 p24 ELISA kit (Clontech), according to the manufacturer's instructions, by Multiskan MK3 (ThermoFisher).

Statistical analysis. Results of the experiments are presented as means ± standard errors of the means (SEM). Student's unpaired *t* test was used to determine significance. A *P* value of <0.05 was considered statistically significant and denoted by an asterisk, while *P* values of <0.01 and <0.001 were represented by two or three asterisks, indicating more and most significant difference, respectively.

ACKNOWLEDGMENTS

We thank the clinicians from the Department of Infectious Diseases of Guangzhou Eighth People's Hospital for recruiting study participants and collecting samples.

The present study was supported by the National Special Research Program of China for Important Infectious Diseases (2018ZX10302103 and 2017ZX10202102), the National Natural Science Foundation of China (81730060 and 81561128007), and the Joint Innovation Program in Healthcare for Special Scientific Research Projects of Guangzhou (201803040002) to H.Z. The present study was also supported by a China Postdoctoral Science Foundation-funded project (2019M663214) to J.C. The funders had no role in study design, data collection and interpretation, or the decision to submit the work for publication.

We have no conflicts of interest to declare.

REFERENCES

1. Chun TW, Stuyver L, Mizell SB, Ehler LA, Mican JA, Baseler M, Lloyd AL, Nowak MA, Fauci AS. 1997. Presence of an inducible HIV-1 latent reservoir during highly active antiretroviral therapy. Proc Natl Acad Sci U S A 94:13193–13197. https://doi.org/10.1073/pnas.94.24.13193.
2. Finzi D, Hermankova M, Pierson T, Carruth LM, Buck C, Chaisson RE, Quinn TC, Chadwick K, Margolick J, Brookmeyer R, Gallant J, Markowitz M, Ho DD, Richman DD, Siliciano RF. 1997. Identification of a reservoir for HIV-1 in patients on highly active antiretroviral therapy. Science 278:1295–1300. https://doi.org/10.1126/science.278.5341.1295.
3. Wong JK, Hezareh M, Gunthard HF, Havlir DV, Ignacio CC, Spina CA, Richman DD. 1997. Recovery of replication-competent HIV despite prolonged suppression of plasma viremia. Science 278:1291–1295. https://doi.org/10.1126/science.278.5341.1291.
4. Siliciano JD, Kajdas J, Finzi D, Quinn TC, Chadwick K, Margolick JB, Kovacs C, Gange SJ, Siliciano RF. 2003. Long-term follow-up studies confirm the stability of the latent reservoir for HIV-1 in resting CD4$^+$ T cells. Nat Med 9:727–728. https://doi.org/10.1038/nm880.
5. Deeks SG. 2012. HIV: shock and kill. Nature 487:439–440. https://doi.org/10.1038/487439a.
6. Archin NM, Liberty AL, Kashuba AD, Choudhary SK, Kuruc JD, Crooks AM, Parker DC, Anderson EM, Kearney MF, Strain MC, Richman DD, Hudgens MG, Bosch RJ, Coffin JM, Eron JJ, Hazuda DJ, Margolis DM. 2012. Administration of vorinostat disrupts HIV-1 latency in patients on antiretroviral therapy. Nature 487:482–485. https://doi.org/10.1038/nature11286.
7. Elliott JH, Wightman F, Solomon A, Ghneim K, Ahlers J, Cameron MJ, Smith MZ, Spelman T, McMahon J, Velayudham P, Brown G, Roney J, Watson J, Prince MH, Hoy JF, Chomont N, Fromentin R, Procopio FA, Zeidan J, Palmer S, Odevall L, Johnstone RW, Martin BP, Sinclair E, Deeks SG, Hazuda DJ, Cameron PU, Sekaly RP, Lewin SR. 2014. Activation of HIV transcription with short-course vorinostat in HIV-infected patients on suppressive antiretroviral therapy. PLoS Pathog 10:e1004473. https://doi.org/10.1371/journal.ppat.1004473.
8. Rasmussen TA, Tolstrup M, Brinkmann CR, Olesen R, Erikstrup C, Solomon A, Winckelmann A, Palmer S, Dinarello C, Buzon M, Lichterfeld M, Lewin SR, Ostergaard L, Sogaard OS. 2014. Panobinostat, a histone deacetylase inhibitor, for latent-virus reactivation in HIV-infected patients on suppressive antiretroviral therapy: a phase 1/2, single group, clinical trial. Lancet HIV 1:e13–e21. https://doi.org/10.1016/S2352-3018(14)70014-1.
9. Søgaard OS, Graversen ME, Leth S, Olesen R, Brinkmann CR, Nissen SK, Kjaer AS, Schleimann MH, Denton PW, Hey-Cunningham WJ, Koelsch KK, Pantaleo G, Krogsgaard K, Sommerfelt M, Fromentin R, Chomont N, Rasmussen TA, Østergaard L, Tolstrup M. 2015. The depsipeptide romidepsin reverses HIV-1 latency in vivo. PLoS Pathog 11:e1005142. https://doi.org/10.1371/journal.ppat.1005142.
10. Marban C, Suzanne S, Dequiedt F, de Walque S, Redel L, Van Lint C, Aunis D, Rohr O. 2007. Recruitment of chromatin-modifying enzymes by CTIP2 promotes HIV-1 transcriptional silencing. EMBO J 26:412–423. https://doi.org/10.1038/sj.emboj.7601516.
11. Keedy KS, Archin NM, Gates AT, Espeseth A, Hazuda DJ, Margolis DM. 2009. A limited group of class I histone deacetylases acts to repress human immunodeficiency virus type 1 expression. J Virol 83:4749–4756. https://doi.org/10.1128/JVI.02585-08.
12. Palmisano I, Della Chiara G, D'Ambrosio RL, Huichalaf C, Brambilla P, Corbetta S, Riba M, Piccirillo R, Valente S, Casari G, Mai A, Martinelli Boneschi F, Gabellini D, Poli G, Schiaffino MV. 2012. Amino acid starvation induces reactivation of silenced transgenes and latent HIV-1 provirus via down-regulation of histone deacetylase 4 (HDAC4). Proc Natl Acad Sci U S A 109:E2284–E2293. https://doi.org/10.1073/pnas.1202174109.
13. Natarajan M, Schiralli LG, Lee C, Missra A, Wasserman GA, Steffen M, Gilmour DS, Henderson AJ. 2013. Negative elongation factor (NELF) coordinates RNA polymerase II pausing, premature termination, and chromatin remodeling to regulate HIV transcription. J Biol Chem 288:25995–26003. https://doi.org/10.1074/jbc.M113.496489.
14. Ruelas DS, Greene WC. 2013. An integrated overview of HIV-1 latency. Cell 155:519–529. https://doi.org/10.1016/j.cell.2013.09.044.
15. Du Chene I, Basyuk E, Lin YL, Triboulet R, Knezevich A, Chable-Bessia C, Mettling C, Baillat V, Reynes J, Corbeau P, Bertrand E, Marcello A, Emiliani S, Kiernan R, Benkirane M. 2007. Suv39H1 and HP1gamma are responsible for chromatin-mediated HIV-1 transcriptional silencing and post-integration latency. EMBO J 26:424–435. https://doi.org/10.1038/sj.emboj.7601517.
16. Imai K, Togami H, Okamoto T. 2010. Involvement of histone H3 lysine 9 (H3K9) methyltransferase G9a in the maintenance of HIV-1 latency and its reactivation by BIX01294. J Biol Chem 285:16538–16545. https://doi.org/10.1074/jbc.M110.103531.
17. Ding D, Qu X, Li L, Zhou X, Liu S, Lin S, Wang P, Liu S, Kong C, Wang X, Liu L, Zhu H. 2013. Involvement of histone methyltransferase GLP in HIV-1 latency through catalysis of H3K9 dimethylation. Virology 440:182–189. https://doi.org/10.1016/j.virol.2013.02.022.
18. Boehm D, Jeng M, Camus G, Gramatica A, Schwarzer R, Johnson JR, Hull PA, Montano M, Sakane N, Pagans S, Godin R, Deeks SG, Krogan NJ, Greene WC, Ott M. 2017. SMYD2-mediated histone methylation contributes to HIV-1 latency. Cell Host Microbe 21:569–579. https://doi.org/10.1016/j.chom.2017.04.011.
19. Ma X, Yang T, Luo Y, Wu L, Jiang Y, Song Z, Pan T, Liu B, Liu G, Liu J, Yu F, He Z, Zhang W, Yang J, Liang L, Guan Y, Zhang X, Li L, Cai W, Tang X, Gao S, Deng K, Zhang H. 2019. TRIM28 promotes HIV-1 latency by SUMOylating CDK9 and inhibiting P-TEFb. Elife 8:e42426. https://doi.org/10.7554/eLife.42426.
20. Taura M, Song E, Ho YC, Iwasaki A. 2019. Apobec3A maintains HIV-1 latency through recruitment of epigenetic silencing machinery to the long terminal repeat. Proc Natl Acad Sci U S A 116:2282–2289. https://doi.org/10.1073/pnas.1819386116.
21. Trojer P, Reinberg D. 2007. Facultative heterochromatin: is there a distinctive molecular signature? Mol Cell 28:1–13. https://doi.org/10.1016/j.molcel.2007.09.011.
22. Sun WW, Jiao S, Sun L, Zhou Z, Jin X, Wang JH. 2018. SUN2 modulates HIV-1 infection and latency through association with lamin A/C to maintain the repressive chromatin. mBio 9:e02408-17. https://doi.org/10.1128/mBio.02408-17.
23. Ma L, Sun L, Jin X, Xiong SD, Wang JH. 2018. Scaffold attachment factor B suppresses HIV-1 infection of CD4(+) T cells by preventing binding of RNA polymerase II to HIV-1's long terminal repeat. J Biol Chem 293:12177–12185. https://doi.org/10.1074/jbc.RA118.002018.
24. Qu D, Sun WW, Li L, Ma L, Sun L, Jin X, Li T, Hou W, Wang JH. 2019. Long noncoding RNA MALAT1 releases epigenetic silencing of HIV-1 replication by displacing the polycomb repressive complex 2 from binding to the LTR promoter. Nucleic Acids Res 47:3013–3027. https://doi.org/10.1093/nar/gkz117.
25. Parker JS, Roe SM, Barford D. 2004. Crystal structure of a PIWI protein suggests mechanisms for siRNA recognition and slicer activity. EMBO J 23:4727–4737. https://doi.org/10.1038/sj.emboj.7600488.
26. Song JJ, Smith SK, Hannon GJ, Joshua-Tor L. 2004. Crystal structure of

Argonaute and its implications for RISC slicer activity. Science 305:1434–1437. https://doi.org/10.1126/science.1102514.
27. Kowalczykiewicz D, Pawlak P, Lechniak D, Wrzesinski J. 2012. Altered expression of porcine Piwi genes and piRNA during development. PLoS One 7:e43816. https://doi.org/10.1371/journal.pone.0043816.
28. Brennecke J, Aravin AA, Stark A, Dus M, Kellis M, Sachidanandam R, Hannon GJ. 2007. Discrete small RNA-generating loci as master regulators of transposon activity in Drosophila. Cell 128:1089–1103. https://doi.org/10.1016/j.cell.2007.01.043.
29. Saito K, Ishizu H, Komai M, Kotani H, Kawamura Y, Nishida KM, Siomi H, Siomi MC. 2010. Roles for the Yb body components Armitage and Yb in primary piRNA biogenesis in Drosophila. Genes Dev 24:2493–2498. https://doi.org/10.1101/gad.1989510.
30. Kojima-Kita K, Kuramochi-Miyagawa S, Nagamori I, Ogonuki N, Ogura A, Hasuwa H, Akazawa T, Inoue N, Nakano T. 2016. MIWI2 as an effector of DNA methylation and gene silencing in embryonic male germ cells. Cell Rep 16:2819–2828. https://doi.org/10.1016/j.celrep.2016.08.027.
31. Aravin A, Gaidatzis D, Pfeffer S, Lagos-Quintana M, Landgraf P, Iovino N, Morris P, Brownstein MJ, Kuramochi-Miyagawa S, Nakano T, Chien M, Russo JJ, Ju J, Sheridan R, Sander C, Zavolan M, Tuschl T. 2006. A novel class of small RNAs bind to MILI protein in mouse testes. Nature 442:203–207. https://doi.org/10.1038/nature04916.
32. Girard A, Sachidanandam R, Hannon GJ, Carmell MA. 2006. A germline-specific class of small RNAs binds mammalian Piwi proteins. Nature 442:199–202. https://doi.org/10.1038/nature04917.
33. Grivna ST, Beyret E, Wang Z, Lin H. 2006. A novel class of small RNAs in mouse spermatogenic cells. Genes Dev 20:1709–1714. https://doi.org/10.1101/gad.1434406.
34. Lau NC, Seto AG, Kim J, Kuramochi-Miyagawa S, Nakano T, Bartel DP, Kingston RE. 2006. Characterization of the piRNA complex from rat testes. Science 313:363–367. https://doi.org/10.1126/science.1130164.
35. Watanabe T, Takeda A, Tsukiyama T, Mise K, Okuno T, Sasaki H, Minami N, Imai H. 2006. Identification and characterization of two novel classes of small RNAs in the mouse germline: retrotransposon-derived siRNAs in oocytes and germline small RNAs in testes. Genes Dev 20:1732–1743. https://doi.org/10.1101/gad.1425706.
36. Malone CD, Brennecke J, Dus M, Stark A, McCombie WR, Sachidanandam R, Hannon GJ. 2009. Specialized piRNA pathways act in germline and somatic tissues of the Drosophila ovary. Cell 137:522–535. https://doi.org/10.1016/j.cell.2009.03.040.
37. Saito K, Inagaki S, Mituyama T, Kawamura Y, Ono Y, Sakota E, Kotani H, Asai K, Siomi H, Siomi MC. 2009. A regulatory circuit for piwi by the large Maf gene traffic jam in Drosophila. Nature 461:1296–1299. https://doi.org/10.1038/nature08501.
38. Keam SP, Young PE, McCorkindale AL, Dang TH, Clancy JL, Humphreys DT, Preiss T, Hutvagner G, Martin DI, Cropley JE, Suter CM. 2014. The human Piwi protein Hiwi2 associates with tRNA-derived piRNAs in somatic cells. Nucleic Acids Res 42:8984–8995. https://doi.org/10.1093/nar/gku620.
39. Zhang X, He X, Liu C, Liu J, Hu Q, Pan T, Duan X, Liu B, Zhang Y, Chen J, Ma X, Zhang X, Luo H, Zhang H. 2016. IL-4 inhibits the biogenesis of an epigenetically suppressive PIWI-interacting RNA to upregulate CD1a molecules on monocytes/dendritic cells. J Immunol 196:1591–1603. https://doi.org/10.4049/jimmunol.1500805.
40. Cichocki F, Lenvik T, Sharma N, Yun G, Anderson SK, Miller JS. 2010. Cutting edge: KIR antisense transcripts are processed into a 28-base PIWI-like RNA in human NK cells. J Immunol 185:2009–2012. https://doi.org/10.4049/jimmunol.1000855.
41. Dharap A, Nakka VP, Vemuganti R. 2011. Altered expression of PIWI RNA in the rat brain after transient focal ischemia. Stroke 42:1105–1109. https://doi.org/10.1161/STROKEAHA.110.598391.
42. Lee EJ, Banerjee S, Zhou H, Jammalamadaka A, Arcila M, Manjunath BS, Kosik KS. 2011. Identification of piRNAs in the central nervous system. RNA 17:1090–1099. https://doi.org/10.1261/rna.2565011.
43. Yan Z, Hu HY, Jiang X, Maierhofer V, Neb E, He L, Hu Y, Hu H, Li N, Chen W, Khaitovich P. 2011. Widespread expression of piRNA-like molecules in somatic tissues. Nucleic Acids Res 39:6596–6607. https://doi.org/10.1093/nar/gkr298.
44. Cheng J, Deng H, Xiao B, Zhou H, Zhou F, Shen Z, Guo J. 2012. piR-823, a novel non-coding small RNA, demonstrates in vitro and in vivo tumor suppressive activity in human gastric cancer cells. Cancer Lett 315:12–17. https://doi.org/10.1016/j.canlet.2011.10.004.
45. Rizzo F, Hashim A, Marchese G, Ravo M, Tarallo R, Nassa G, Giurato G, Rinaldi A, Cordella A, Persico M, Sulas P, Perra A, Ledda-Columbano GM, Columbano A, Weisz A. 2014. Timed regulation of P-element-induced wimpy testis-interacting RNA expression during rat liver regeneration. Hepatology 60:798–806. https://doi.org/10.1002/hep.27267.
46. He X, Chen X, Zhang X, Duan X, Pan T, Hu Q, Zhang Y, Zhong F, Liu J, Zhang H, Luo J, Wu K, Peng G, Luo H, Zhang L, Li X, Zhang H. 2015. An Lnc RNA (GAS5)/SnoRNA-derived piRNA induces activation of TRAIL gene by site-specifically recruiting MLL/COMPASS-like complexes. Nucleic Acids Res 43:3712–3725. https://doi.org/10.1093/nar/gkv214.
47. Yu T, Koppetsch BS, Pagliarani S, Johnston S, Silverstein NJ, Luban J, Chappell K, Weng Z, Theurkauf WE. 2019. The piRNA response to retroviral invasion of the koala genome. Cell 179:632–643. https://doi.org/10.1016/j.cell.2019.09.002.
48. Sugimoto K, Kage H, Aki N, Sano A, Kitagawa H, Nagase T, Yatomi Y, Ohishi N, Takai D. 2007. The induction of H3K9 methylation by PIWIL4 at the p16Ink4a locus. Biochem Biophys Res Commun 359:497–502. https://doi.org/10.1016/j.bbrc.2007.05.136.
49. Ponnusamy M, Yan KW, Liu CY, Li PF, Wang K. 2017. PIWI family emerging as a decisive factor of cell fate: an overview. Eur J Cell Biol 96:746–757. https://doi.org/10.1016/j.ejcb.2017.09.004.
50. Zhong F, Zhou N, Wu K, Guo Y, Tan W, Zhang H, Zhang X, Geng G, Pan T, Luo H, Zhang Y, Xu Z, Liu J, Liu B, Gao W, Liu C, Ren L, Li J, Zhou J, Zhang H. 2015. A SnoRNA-derived piRNA interacts with human interleukin-4 pre-mRNA and induces its decay in nuclear exosomes. Nucleic Acids Res 43:10474–10491. https://doi.org/10.1093/nar/gkv954.
51. Rajasethupathy P, Antonov I, Sheridan R, Frey S, Sander C, Tuschl T, Kandel ER. 2012. A role for neuronal piRNAs in the epigenetic control of memory-related synaptic plasticity. Cell 149:693–707. https://doi.org/10.1016/j.cell.2012.02.057.
52. Sienski G, Donertas D, Brennecke J. 2012. Transcriptional silencing of transposons by Piwi and maelstrom and its impact on chromatin state and gene expression. Cell 151:964–980. https://doi.org/10.1016/j.cell.2012.10.040.
53. Szmulewicz MN, Novick GE, Herrera RJ. 1998. Effects of Alu insertions on gene function. Electrophoresis 19:1260–1264. https://doi.org/10.1002/elps.1150190806.
54. Kazazian HJ. 2004. Mobile elements: drivers of genome evolution. Science 303:1626–1632. https://doi.org/10.1126/science.1089670.
55. Wu D, Fu H, Zhou H, Su J, Zhang F, Shen J. 2015. Effects of novel ncRNA molecules, p15-piRNAs, on the methylation of DNA and histone H3 of the CDKN2B promoter region in U937 cells. J Cell Biochem 116:2744–2754. https://doi.org/10.1002/jcb.25199.
56. Hwang YE, Baek YM, Baek A, Kim DE. 2019. Oxidative stress causes Alu RNA accumulation via PIWIL4 sequestration into stress granules. BMB Rep 52:196–201. https://doi.org/10.5483/BMBRep.2019.52.3.146.
57. Peterlin BM, Liu P, Wang X, Cary D, Shao W, Leoz M, Hong T, Pan T, Fujinaga K. 2017. Hili inhibits HIV replication in activated T cells. J Virol 91:e00237-17. https://doi.org/10.1128/JVI.00237-17.
58. Platt EJ, Wehrly K, Kuhmann SE, Chesebro B, Kabat D. 1998. Effects of CCR5 and CD4 cell surface concentrations on infections by macrophagetropic isolates of human immunodeficiency virus type 1. J Virol 72:2855–2864. https://doi.org/10.1128/JVI.72.4.2855-2864.1998.
59. Wei X, Decker JM, Liu H, Zhang Z, Arani RB, Kilby JM, Saag MS, Wu X, Shaw GM, Kappes JC. 2002. Emergence of resistant human immunodeficiency virus type 1 in patients receiving fusion inhibitor (T-20) monotherapy. Antimicrob Agents Chemother 46:1896–1905. https://doi.org/10.1128/aac.46.6.1896-1905.2002.
60. Kamori D, Ueno T. 2017. HIV-1 Tat and viral latency: what we can learn from naturally occurring sequence variations. Front Microbiol 8:80. https://doi.org/10.3389/fmicb.2017.00080.
61. Garber ME, Jones KA. 1999. HIV-1 Tat: coping with negative elongation factors. Curr Opin Immunol 11:460–465. https://doi.org/10.1016/S0952-7915(99)80077-6.
62. Parada CA, Roeder RG. 1996. Enhanced processivity of RNA polymerase II triggered by Tat-induced phosphorylation of its carboxy-terminal domain. Nature 384:375–378. https://doi.org/10.1038/384375a0.
63. Spina CA, Anderson J, Archin NM, Bosque A, Chan J, Famiglietti M, Greene WC, Kashuba A, Lewin SR, Margolis DM, Mau M, Ruelas D, Saleh S, Shirakawa K, Siliciano RF, Singhania A, Soto PC, Terry VH, Verdin E, Woelk C, Wooden S, Xing S, Planelles V. 2013. An in-depth comparison of latent HIV-1 reactivation in multiple cell model systems and resting CD4$^+$ T cells from aviremic patients. PLoS Pathog 9:e1003834. https://doi.org/10.1371/journal.ppat.1003834.
64. Li J, Chen C, Ma X, Geng G, Liu B, Zhang Y, Zhang S, Zhong F, Liu C, Yin Y, Cai W, Zhang H. 2016. Long noncoding RNA NRON contributes to

HIV-1 latency by specifically inducing tat protein degradation. Nat Commun 7:11730. https://doi.org/10.1038/ncomms11730.
65. Kauder SE, Bosque A, Lindqvist A, Planelles V, Verdin E. 2009. Epigenetic regulation of HIV-1 latency by cytosine methylation. PLoS Pathog 5:e1000495. https://doi.org/10.1371/journal.ppat.1000495.
66. Jordan A, Bisgrove D, Verdin E. 2003. HIV reproducibly establishes a latent infection after acute infection of T cells in vitro. EMBO J 22:1868–1877. https://doi.org/10.1093/emboj/cdg188.
67. Bullen CK, Laird GM, Durand CM, Siliciano JD, Siliciano RF. 2014. New ex vivo approaches distinguish effective and ineffective single agents for reversing HIV-1 latency in vivo. Nat Med 20:425–429. https://doi.org/10.1038/nm.3489.
68. Archin NM, Sung JM, Garrido C, Soriano-Sarabia N, Margolis DM. 2014. Eradicating HIV-1 infection: seeking to clear a persistent pathogen. Nat Rev Microbiol 12:750–764. https://doi.org/10.1038/nrmicro3352.
69. Colin L, Van Lint C. 2009. Molecular control of HIV-1 postintegration latency: implications for the development of new therapeutic strategies. Retrovirology 6:111. https://doi.org/10.1186/1742-4690-6-111.
70. Ma JB, Ye K, Patel DJ. 2004. Structural basis for overhang-specific small interfering RNA recognition by the PAZ domain. Nature 429:318–322. https://doi.org/10.1038/nature02519.
71. Lingel A, Simon B, Izaurralde E, Sattler M. 2004. Nucleic acid 3′-end recognition by the Argonaute2 PAZ domain. Nat Struct Mol Biol 11:576–577. https://doi.org/10.1038/nsmb777.
72. Klenov MS, Sokolova OA, Yakushev EY, Stolyarenko AD, Mikhaleva EA, Lavrov SA, Gvozdev VA. 2011. Separation of stem cell maintenance and transposon silencing functions of Piwi protein. Proc Natl Acad Sci U S A 108:18760–18765. https://doi.org/10.1073/pnas.1106676108.
73. Nguyen K, Das B, Dobrowolski C, Karn J. 2017. Multiple histone lysine methyltransferases are required for the establishment and maintenance of HIV-1 latency. mBio 8:e00133-17. https://doi.org/10.1128/mBio.00133-17.
74. Barski A, Cuddapah S, Cui K, Roh TY, Schones DE, Wang Z, Wei G, Chepelev I, Zhao K. 2007. High-resolution profiling of histone methylations in the human genome. Cell 129:823–837. https://doi.org/10.1016/j.cell.2007.05.009.
75. Guillemette B, Drogaris P, Lin HH, Armstrong H, Hiragami-Hamada K, Imhof A, Bonneil E, Thibault P, Verreault A, Festenstein RJ. 2011. H3 lysine 4 is acetylated at active gene promoters and is regulated by H3 lysine 4 methylation. PLoS Genet 7:e1001354. https://doi.org/10.1371/journal.pgen.1001354.
76. Zhang Y, Zheng X, Tan H, Lu Y, Tao D, Liu Y, Ma Y. 2018. PIWIL2 suppresses Siah2-mediated degradation of HDAC3 and facilitates CK2alpha-mediated HDAC3 phosphorylation. Cell Death Dis 9:423. https://doi.org/10.1038/s41419-018-0462-8.
77. van Praag RM, Prins JM, Roos MT, Schellekens PT, Ten BI, Yong SL, Schuitemaker H, Eerenberg AJ, Jurriaans S, de Wolf F, Fox CH, Goudsmit J, Miedema F, Lange JM. 2001. OKT3 and IL-2 treatment for purging of the latent HIV-1 reservoir in vivo results in selective long-lasting CD4$^+$ T cell depletion. J Clin Immunol 21:218–226. https://doi.org/10.1023/a:1011091300321.
78. Stellbrink H-J, van Lunzen J, Westby M, O'Sullivan E, Schneider C, Adam A, Weitner L, Kuhlmann B, Hoffmann C, Fenske S, Aries PS, Degen O, Eggers C, Petersen H, Haag F, Horst HA, Dalhoff K, Möcklinghoff C, Cammack N, Tenner-Racz K, Racz P. 2002. Effects of interleukin-2 plus highly active antiretroviral therapy on HIV-1 replication and proviral DNA (COSMIC trial). AIDS 16:1479–1487. https://doi.org/10.1097/00002030-200207260-00004.
79. Kulkosky J, Nunnari G, Otero M, Calarota S, Dornadula G, Zhang H, Malin A, Sullivan J, Xu Y, DeSimone J, Babinchak T, Stern J, Cavert W, Haase A, Pomerantz RJ. 2002. Intensification and stimulation therapy for human immunodeficiency virus type 1 reservoirs in infected persons receiving virally suppressive highly active antiretroviral therapy. J Infect Dis 186:1403–1411. https://doi.org/10.1086/344357.
80. Xing S, Siliciano RF. 2013. Targeting HIV latency: pharmacologic strategies toward eradication. Drug Discov Today 18:541–551. https://doi.org/10.1016/j.drudis.2012.12.008.
81. Marks PA. 2007. Discovery and development of SAHA as an anticancer agent. Oncogene 26:1351–1356. https://doi.org/10.1038/sj.onc.1210204.
82. Sobala A, Hutvagner G. 2013. Small RNAs derived from the 5′ end of tRNA can inhibit protein translation in human cells. RNA Biol 10:553–563. https://doi.org/10.4161/rna.24285.
83. Anderson P, Ivanov P. 2014. tRNA fragments in human health and disease. FEBS Lett 588:4297–4304. https://doi.org/10.1016/j.febslet.2014.09.001.
84. Wang Q, Lee I, Ren J, Ajay SS, Lee YS, Bao X. 2013. Identification and functional characterization of tRNA-derived RNA fragments (tRFs) in respiratory syncytial virus infection. Mol Ther 21:368–379. https://doi.org/10.1038/mt.2012.237.
85. Saikia M, Krokowski D, Guan BJ, Ivanov P, Parisien M, Hu GF, Anderson P, Pan T, Hatzoglou M. 2012. Genome-wide identification and quantitative analysis of cleaved tRNA fragments induced by cellular stress. J Biol Chem 287:42708–42725. https://doi.org/10.1074/jbc.M112.371799.
86. Kumar P, Kuscu C, Dutta A. 2016. Biogenesis and function of transfer RNA-related fragments (tRFs). Trends Biochem Sci 41:679–689. https://doi.org/10.1016/j.tibs.2016.05.004.
87. Ruggero K, Guffanti A, Corradin A, Sharma VK, De Bellis G, Corti G, Grassi A, Zanovello P, Bronte V, Ciminale V, D'Agostino DM. 2014. Small noncoding RNAs in cells transformed by human T-cell leukemia virus type 1: a role for a tRNA fragment as a primer for reverse transcriptase. J Virol 88:3612–3622. https://doi.org/10.1128/JVI.02823-13.
88. Martin M, Kettmann R, Dequiedt F. 2009. Class IIa histone deacetylases: conducting development and differentiation. Int J Dev Biol 53:291–301. https://doi.org/10.1387/ijdb.082698mm.
89. Grozinger CM, Hassig CA, Schreiber SL. 1999. Three proteins define a class of human histone deacetylases related to yeast Hda1p. Proc Natl Acad Sci U S A 96:4868–4873. https://doi.org/10.1073/pnas.96.9.4868.
90. Lee HA, Song MJ, Seok YM, Kang SH, Kim SY, Kim I. 2015. Histone deacetylase 3 and 4 complex stimulates the transcriptional activity of the mineralocorticoid receptor. PLoS One 10:e0136801. https://doi.org/10.1371/journal.pone.0136801.
91. Hohl M, Wagner M, Reil JC, Muller SA, Tauchnitz M, Zimmer AM, Lehmann LH, Thiel G, Bohm M, Backs J, Maack C. 2013. HDAC4 controls histone methylation in response to elevated cardiac load. J Clin Investig 123:1359–1370. https://doi.org/10.1172/JCI61084.
92. Bannister AJ, Kouzarides T. 2011. Regulation of chromatin by histone modifications. Cell Res 21:381–395. https://doi.org/10.1038/cr.2011.22.
93. Stephens AD, Liu PZ, Banigan EJ, Almassalha LM, Backman V, Adam SA, Goldman RD, Marko JF. 2018. Chromatin histone modifications and rigidity affect nuclear morphology independent of lamins. Mol Biol Cell 29:220–233. https://doi.org/10.1091/mbc.E17-06-0410.
94. Rousseaux MW, Revelli J-P, Vázquez-Vélez GE, Kim J-Y, Craigen E, Gonzales K, Beckinghausen J, Zoghbi HY. 2018. Depleting Trim28 in adult mice is well tolerated and reduces levels of alpha-synuclein and tau. Elife 7:e36768. https://doi.org/10.7554/eLife.36768.
95. Hsieh TH, Hsu CY, Tsai CF, Long CY, Chai CY, Hou MF, Lee JN, Wu DC, Wang SC, Tsai EM. 2015. miR-125a-5p is a prognostic biomarker that targets HDAC4 to suppress breast tumorigenesis. Oncotarget 6:494–509. https://doi.org/10.18632/oncotarget.2674.
96. Wu H, Liu C, Yang Q, Xin C, Du J, Sun F, Zhou L. 2019. MIR145-3p promotes autophagy and enhances bortezomib sensitivity in multiple myeloma by targeting HDAC4. Autophagy 16:683–697. https://doi.org/10.1080/15548627.2019.1635380.
97. Yamashita M, Emerman M. 2004. Capsid is a dominant determinant of retrovirus infectivity in nondividing cells. J Virol 78:5670–5678. https://doi.org/10.1128/JVI.78.11.5670-5678.2004.
98. Liu B, Zou F, Lu L, Chen C, He D, Zhang X, Tang X, Liu C, Li L, Zhang H. 2016. Chimeric antigen receptor T cells guided by the single-chain Fv of a broadly neutralizing antibody specifically and effectively eradicate virus reactivated from latency in CD4$^+$ T lymphocytes isolated from HIV-1-infected individuals receiving suppressive combined antiretroviral therapy. J Virol 90:9712–9724. https://doi.org/10.1128/JVI.00852-16.
99. Zhang J, Huang F, Tan L, Bai C, Chen B, Liu J, Liang J, Liu C, Zhang S, Lu G, Chen Y, Zhang H. 2016. Host protein moloney leukemia virus 10 (MOV10) acts as a restriction factor of influenza A virus by inhibiting the nuclear import of the viral nucleoprotein. J Virol 90:3966–3980. https://doi.org/10.1128/JVI.03137-15.
100. Siliciano JD, Siliciano RF. 2005. Enhanced culture assay for detection and quantitation of latently infected, resting CD4$^+$ T-cells carrying replication-competent virus in HIV-1-infected individuals. Methods Mol Biol 304:3–15. https://doi.org/10.1385/1-59259-907-9:003.